communications biology

Article

https://doi.org/10.1038/s42003-024-06771-9

Reversible control of kinase signaling through chemical-induced dephosphorylation

Check for updates

Ying Sun[1,2], Rihong Zhou[2], Jin Hu[2], Shan Feng[2] & Qi Hu[2,3]

The coordination between kinases and phosphatases is crucial for regulating the phosphorylation levels of essential signaling molecules. Methods enabling precise control of kinase activities are valuable for understanding the kinase functions and for developing targeted therapies. Here, we use the abscisic acid (ABA)-induced proximity system to reversibly control kinase signaling by recruiting phosphatases. Using this method, we found that the oncogenic tyrosine kinase BCR::ABL1 can be inhibited by recruiting various cytoplasmic phosphatases. We also discovered that the oncogenic serine/threonine kinase BRAF(V600E), which has been reported to bypass phosphorylation regulation, can be positively regulated by protein phosphatase 1 (PP1) and negatively regulated by PP5. Additionally, we observed that the dual-specificity kinase MEK1 can be inhibited by recruiting PP5. This suggests that bifunctional molecules capable of recruiting PP5 to MEK or RAF kinases could be promising anticancer drug candidates. Thus, the ABA-induced dephosphorylation method enables rapid screening of phosphatases to precisely control kinase signaling.

Kinases and phosphatases regulate growth, differentiation and other essential cellular processes[1]. Protein kinases usually function as signal transducers by receiving activating signals from upstream ligands or regulators and catalyzing the phosphorylation of downstream substrate proteins; in contrast, phosphatases counteract the functions of kinases by catalyzing the dephosphorylation reaction. In human, more than 500 protein kinases and nearly 200 protein phosphatases have been identified[2,3]. Dysregulation of kinases and phosphatases contributes to the development of diseases such as cancers[4], neurodegenerative diseases[5], and metabolic diseases[6]. How the protein kinases and phosphatases coordinate to maintain the phosphorylation of substrate proteins at proper levels is always a focus of kinase/phosphatase related studies.

In addition to sharing the same substrates, protein kinases and phosphatases also regulate the enzymatic activities of each other. In particular, the activities of protein kinases are tightly controlled by phosphorylation and dephosphorylation. For example, the oncogenic kinase BCR-ABL1, which is encoded by the fusion gene *BCR-ABL1* that is found in most chronic myelogenous leukemia (CML) patients, requires phosphorylation of its activation loop to be activated[7]. Following the recommendations from the HUGO Gene Nomenclature Committee (HGNC) to describe gene fusions[8], we use the name BCR::ABL1 instead of BCR-ABL1 in this study. The RAF kinases, including CRAF, ARAF and BRAF, represent kinases that are regulated by more complicated phosphorylation and dephosphorylation processes[9]. Phosphorylation of BRAF at S365 inhibited the kinase activity, while phosphorylation at S729 promotes the activation of BRAF[9].

Manipulating the phosphorylation and dephosphorylation of protein kinases or their substrates is a promising strategy to regulate the kinase signaling pathways. Lim et al. showed that the catalytic domain of a tyrosine phosphatase SHP1 with its N terminus fused to the ABL binding domain (ABD) of RIN1 could dephosphorylate BCR::ABL1 to inhibit its oncogenic activity[10]. Similarly, Simpson et al. reported that phosphatases fused to an anti-GFP nanobody could bind to GFP-fused target proteins and dephosphorylate the target proteins[11].

Inspired by proteolysis targeting chimeras (PROTACs)[12], which consist of a binder or inhibitor of the target protein, a binder or activator of an E3 ubiquitin ligase, and a linker covalently linked the two binders, Yamazoe et al. developed phosphatase recruiting chimeras (PhoRCs) by covalently linking a binder of the target protein with a binder or activator of a phosphatase, and demonstrated that PHORCs effectively inhibited AKT by recruiting protein phosphatase 1 (PP1) to dephosphorylate AKT[13]. The same strategy has been used to design heterobifunctional molecules that dephosphorylated Tau by recruiting protein phosphatase 2 A (PP2A)[14], dephosphorylated FOXO3a by PP2A[15], and that dephosphorylated ASK1 by protein phosphatase 5 (PP5)[16], highlighting the therapeutic potential of

[1]Zhejiang University, Hangzhou, Zhejiang, China. [2]Key Laboratory of Structural Biology of Zhejiang Province, School of Life Sciences, Westlake University; Institute of Biology, Westlake Institute for Advanced Study, Hangzhou, Zhejiang, China. [3]Westlake AI Therapeutics Lab, Westlake Laboratory of Life Sciences and Biomedicine, Hangzhou, Zhejiang, China. e-mail: huqi@westlake.edu.cn

the PHORC strategy. But given the large number of protein kinases and phosphatases and their complicated regulatory mechanisms, a key question for the PHORC strategy is which phosphatase should be chosen to dephosphorylate a given target protein.

In this study, using the chemically induced proximity (CIP) strategy we develop a method to quickly screen phosphatases to precisely control kinase signaling. The basic idea of the CIP strategy is to use a chemical to induce the proximity of two or more molecules, especially biomacromolecules[17]. Several CIP systems have been identified[17]. For example, the rapamycin-induced dimerization system has been widely used in biological studies, such as to regulate gene expression[18], and protein translocation[19,20]. However, the interference of rapamycin with mTOR and FKBP12 limits its application. In contrast, the plant hormone abscisic acid (ABA) induced proximity system, in which ABA induces the binding of plant PYR1/PYL/RCAR proteins (PYLs) to a plant phosphatase ABI1, has the advantage of not interacting with proteins in mammalian cells[21]. ABA has good stability and bioavailability, and lower toxicity in mammalian cells[21]. A point mutation—D143A was introduced into ABI1 to disrupt the phosphatase activity of ABI1[21]. We fused the D143A mutant of ABI1 to the N or C termini of kinases, fused PYL2 to the N or C termini of phosphatases, and then used ABA to induce the proximity of the kinases and phosphatases. We demonstrated that the ABA induced proximity system can be used to reversibly control both tyrosine kinases (BCR::ABL1 as an example) and serine/threonine kinases (BRAF-MEK-ERK pathway as an example). Using this method, we identified phosphatases that can be recruited to regulate BCR::ABL1, BRAF(V600E) and MEK1.

Results

The ABA induced proximity system can reversibly control BCR::ABL1 signaling

To test whether the ABA induced proximity system can be used to control tyrosine kinases, we chose BCR::ABL1 as an example. ABL1 contains a Src homology 3 (SH3) domain, a Src homology 2 (SH2) domain and a catalytic domain; in its unphosphorylated state, ABL1 has its catalytic domain inhibited by the SH2 and SH3 domains; fusion of the BCR (breakpoint cluster region) protein to the N-terminus of ABL1 leads to the dimerization and phosphorylation of BCR::ABL1, resulting in the release of the SH2 and SH3 domains from the catalytic domain and constitutive activation of ABL1. As for the phosphatase, we chose the tyrosine phosphatase SHP1 that has been reported to inhibit the function of BCR::ABL1. By fusing a His-tagged PYL2 (residues 11 to 188) to the N terminus of SHP1 and by fusing a FLAG-tagged ABI (ABI1, residues 126 to 422, with the D143A mutation) to the N terminus of BCR::ABL1, we created two chimeric proteins His-PYL2-SHP1 and FLAG-ABI-BCR::ABL1 (Fig. 1a).

We overexpressed the two chimeric proteins and purified them to homogeneity. First, we confirmed that ABA can induce the interaction between His-PYL2-SHP1 and FLAG-ABI-BCR::ABL1 using a gel filtration assay (Supplementary Fig. 1). Next, we assessed the impact of His-

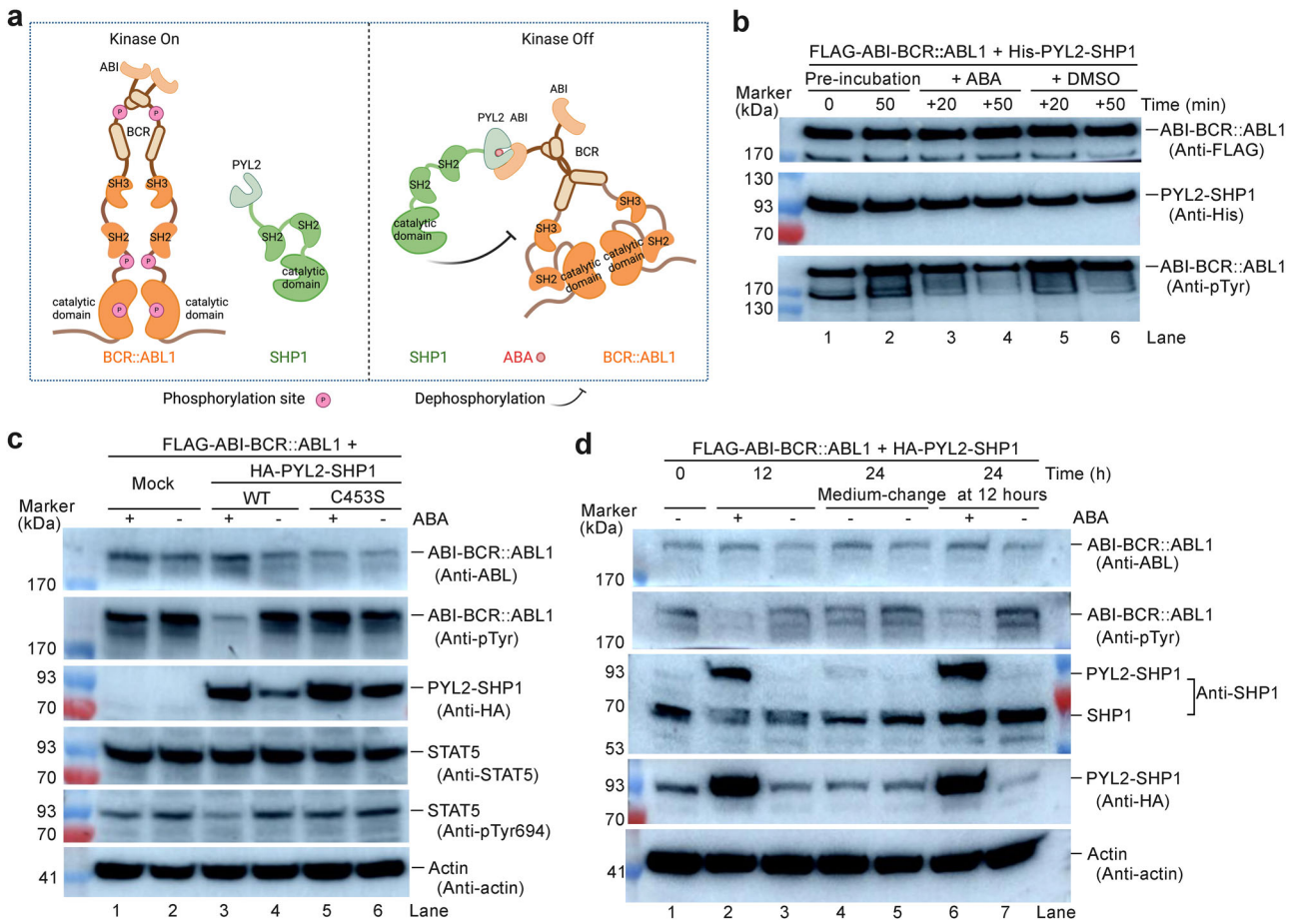

Fig. 1 | Recruitment of SHP1 to BCR::ABL1 dephosphorylated BCR::ABL1 and inhibited its activity to phosphorylate STAT5. a Illustration of the ABA induced proximity system. ABI (residues 126-422, D143A) and PYL2 (residues 11-188) are fused to the N termini of BCR::ABL1 and SHP1, respectively. ABA induces the dimerization of PYL2 with ABI to bring SHP1 close to BCR::ABL1. Created with BioRender.com. **b** The purified FLAG-tagged ABI-BCR::ABL1 could be phosphorylated by itself and dephosphorylated by recruiting His-tagged PYL2-SHP1 to it. **c** In Ba/F3 cells, recruitment of HA-tagged PYL2-SHP1 decreased the phosphorylation level of FLAG-tagged ABI-BCR::ABL1 and inhibited the phosphorylation of STAT5 at Y694. **d** The decreased phosphorylation level of FLAG-tagged ABI-BCR::ABL1 by recruiting HA-tagged PYL2-SHP1 in Ba/F3 cells was recovered after ABA was withdraw.

PYL2-SHP1 on the autophosphorylation level of FLAG-ABI-BCR::ABL1. After incubation of the purified His-PYL2-SHP1 with FLAG-ABI-BCR::ABL1 in a kinase reaction buffer for 50 min, an increase of the tyrosine phosphorylation (pTyr) level of FLAG-ABI-BCR::ABL1 was observed (Fig. 1b, lanes 1 vs. 2). Then half of the reaction was incubated with ABA while the other half was incubated with DMSO for additional 20 or 50 min. Upon addition of ABA but not DMSO, the pTyr level of BCR::ABL1 sharply decreased (Fig. 1b, lanes 3 to 6), suggesting that recruitment of SHP1 to BCR::ABL1 by the ABA induced proximity system can promote the dephosphorylation of BCR::ABL1.

Next, we tested whether the ABA induced proximity system can control BCR::ABL1 signaling in Ba/F3 cells. Ba/F3 cells are a murine pro-B cell line frequently used in the study of oncogenic kinases due to their dependence on interleukin-3 (IL-3) for survival, which can be overridden by oncogenic mutations in the kinases[22]. We stably expressed FLAG-tagged ABI-BCR::ABL1 alone or together with HA-tagged PYL2-SHP1 in Ba/F3 cells. When expressed together with wild-type PYL2-SHP1 but not expressed alone or expressed together with PYL2-SHP1 carrying a catalytic-dead mutation C453S in SHP1, ABI-BCR::ABL1 had its pTyr level decreased upon treatment with ABA (Fig. 1c). The pTyr level of STAT5, which is an important substrate of BCR::ABL1, was also decreased by the recruitment of SHP1 to BCR::ABL1 (Fig. 1c, lanes 3 vs. 4).

In addition to STAT5, BCR::ABL1 has also been reported to be able to activate the PI3K/AKT and MAPK/ERK pathways[23], and catalyze the phosphorylation of the SH2/SH3 domain-containing protein CrkL[24]. Therefore, we also checked changes in the phosphorylation levels of AKT, ERK and CrkL in Ba/F3 cells upon treatment with ABA or imatinib (IMA). IMA is a small molecule inhibitor of BCR::ABL1 and has been approved for the treatment of CML[25]. In contrast to the obvious decrease in the phosphorylation level of STAT5, the phosphorylation levels of AKT, ERK, and CrkL showed little or moderate change upon treatment with ABA or IMA for 12 h (Supplementary Fig. 2).

The decrease of pTyr level of BCR::ABL1 is reversible. In Ba/F3 cells stably expressing both ABI-BCR::ABL1 and PYL2-SHP1, after 12-hour treatment with ABA, the pTyr level of BCR::ABL1 was decreased (Fig. 1d, lanes 2 vs. 3). Then for half of the cells, the medium was changed to fresh medium not containing ABA, and after additional 12 hours, the pTyr level of BCR::ABL1 was recovered (Fig. 1d, lane 4); in the other half of the cells of which the medium was changed to fresh medium containing ABA, the pTyr level of BCR::ABL1 was still very low after additional 12 hours (Fig. 1d, lane 6). These results suggest that the ABA induced proximity system can reversibly control BCR::ABL1 signaling in Ba/F3 cells.

ABA can increase the protein level of PYL2 fusion proteins

Unexpectedly, we found that the protein level of PYL2-SHP1 was increased upon treatment with ABA (Fig. 1c, lanes 3 and 5; Fig. 1d, lanes 2 and 6). A similar result was also observed when PYL2-SHP1 was co-expressed with FLAG-tagged ABI (Supplementary Fig. 3a) or with BCR::ABL1 (Supplementary Fig. 3b). But when the interaction between PYL2 and ABA was disrupted by introducing a K64A mutation into PYL2, adding ABA could no longer increase the protein level of PYL2-SHP1 (Supplementary Fig. 3c). Even if there was no SHP1 fused to PYL2, adding ABA could still increase the protein level of PYL2 (Supplementary Fig. 3d). We conclude that the ABA induced upregulation of PYL2-SHP1 was not because of the function of BCR::ABL1, SHP1, or the interaction between ABI and PYL2, but because of the binding of ABA to PYL2. This unexpected stabilizing effect of ABA binding further adds to the inducibility of this CIP system.

To test whether the degradation of PYL2 occurs through the ubiquitin-proteasome pathway, we treated the Ba/F3 cells with MG132, a proteasome inhibitor[26]. Unexpectedly, MG132 treatment decreased the protein levels of both FLAG-tagged ABI-BCR::ABL1 and HA-tagged PYL2-SHP1 (Supplementary Fig. 3e). Previous studies also found that the protein level of BCR::ABL1 decreased upon MG132 treatment, but the reason is unclear[27,28].

Screening of phosphatases to regulate BCR::ABL1 phosphorylation

In addition to SHP1, we speculate whether other phosphatases can also be used to regulate BCR::ABL1 phosphorylation. The human protein phosphatases, which can be divided into serine/threonine phosphatases (PSPs), tyrosine phosphatases (PTPs), and dual-specificity phosphatases (DUSPs), have various subcellular locations. We selected several representative phosphatases to test using the ABA induced proximity system (Fig. 2a).

The first type of phosphatases we tested are PTPs. SHP1 and a cytosolic variant of PTPN5 (also called STEP, STriatal-Enriched protein tyrosine Phosphatase) are cytosolic PTPs; PTP1B and TCPTP are also PTPs, but are localized to the endoplasmic reticulum (ER). Previous studies have showed that PTP1B can dephosphorylate BCR::ABL1 at Tyr1086 to stabilize BCR::ABL1[29]. We fused HA-tagged PYL2 to the N or C termini of these phosphatases, and stably expressed them together with FLAG-tagged ABI-BCR::ABL1 in Ba/F3 cells. After 12-hour treatment with ABA, a significant decrease of the pTyr level of FLAG-ABI-BCR::ABL1 was observed in Ba/F3 cells expressing HA-PYL2-SHP1, HA-PYL2-PTPN5, PTPN5-PYL2-HA, HA-PYL2-PTP1B, PTP1B-PYL2-HA, or HA-PYL2-TCPTP (Fig. 2b, c).

Next, we tested DUSPs, which can dephosphorylate a variety of substrates including protein tyrosine, threonine, and serine residues, and phosphoinositides[30]. We chose PTEN and DUSP9 as representatives of cytosolic DUSPs, and DUSP4 and DUSP5 as representatives of DUSPs in the nucleus. PTEN prefers phosphatidylinositol (3,4,5)-trisphosphate (PIP_3) as its substrate, but can also dephosphorylate proteins[31]. DUSP9 has been reported to dephosphorylate mitogen-activated protein kinases (MAPKs)[32]. DUSP4 and DUSP5 are known to dephosphorylate extracellular signal-regulated kinases (ERKs) in nucleus[33]. We found that only PTEN and DUSP9 with HA-tagged PYL2 fused to their N termini decreased the pTyr level of ABI-BCR::ABL1 upon treatment with ABA (Fig. 2c, d).

Lastly, we tested three cytosolic PSPs, including PP1, PP2A, and PP5. A previous study showed that recruiting PP1 to EGFR reduced the phosphorylation level of EGFR at Y1068, suggesting that PSPs could be promiscuous in dephosphorylating tyrosine residues[13]. We found that only recruitment of PP5 induced the dephosphorylation of BCR::ABL1 (Fig. 2e).

By using catalytic-dead mutants of PTPN5, PTP1B, TCPTP, and PTEN as controls, we demonstrated that the effects of recruiting these phosphatases to BCR::ABL1 on the pTyr level of BCR::ABL1 depend on the catalytic activities of these phosphatases (Supplementary Fig. 4). For PTPN5, recruitment of its catalytic-dead mutant to BCR::ABL1 also decreased the pTyr level of BCR::ABL1, though the decrease was not as significant as that caused by recruitment of active PTPN5, indicating that non-catalytic effect of PTPN5 also contributes to its inhibitory activity against BCR::ABL1 phosphorylation.

We next tested the effect of ABA on the cell viability of Ba/F3 cells stably expressing both FLAG-tagged ABI-BCR::ABL1 and HA-tagged PYL2-phosphatase fusion proteins. ABA had the highest activity in Ba/F3 cells expressing HA-PYL2-PTPN5 (Fig. 2f, g), with an IC_{50} value of 1.4 μM (Fig. 2h).

The above results show that PTPs and DUSPs in cytoplasm can dephosphorylate BCR::ABL1 when they are recruited to BCR::ABL1 through the ABA induced proximity system. Only when PYL2 was fused to the N termini but not C termini of SHP1, TCPTP, PTEN, and DUSP9, recruitment of these phosphatases to BCR::ABL1 dephosphorylated BCR::ABL1, indicating that the position and orientation of phosphatases relative to kinases should be taken into consideration when the ABA induced proximity system is used to control kinase signaling pathways. Regarding the phosphatases that fail to dephosphorylate BCR::ABL1, we cannot rule out the possibility that this is due to an improper distance or orientation between these phosphatases and BCR::ABL1 when brought together. Alternatively, it may be because of direct interference with the phosphatase activities caused by the fused HA-tagged PYL2.

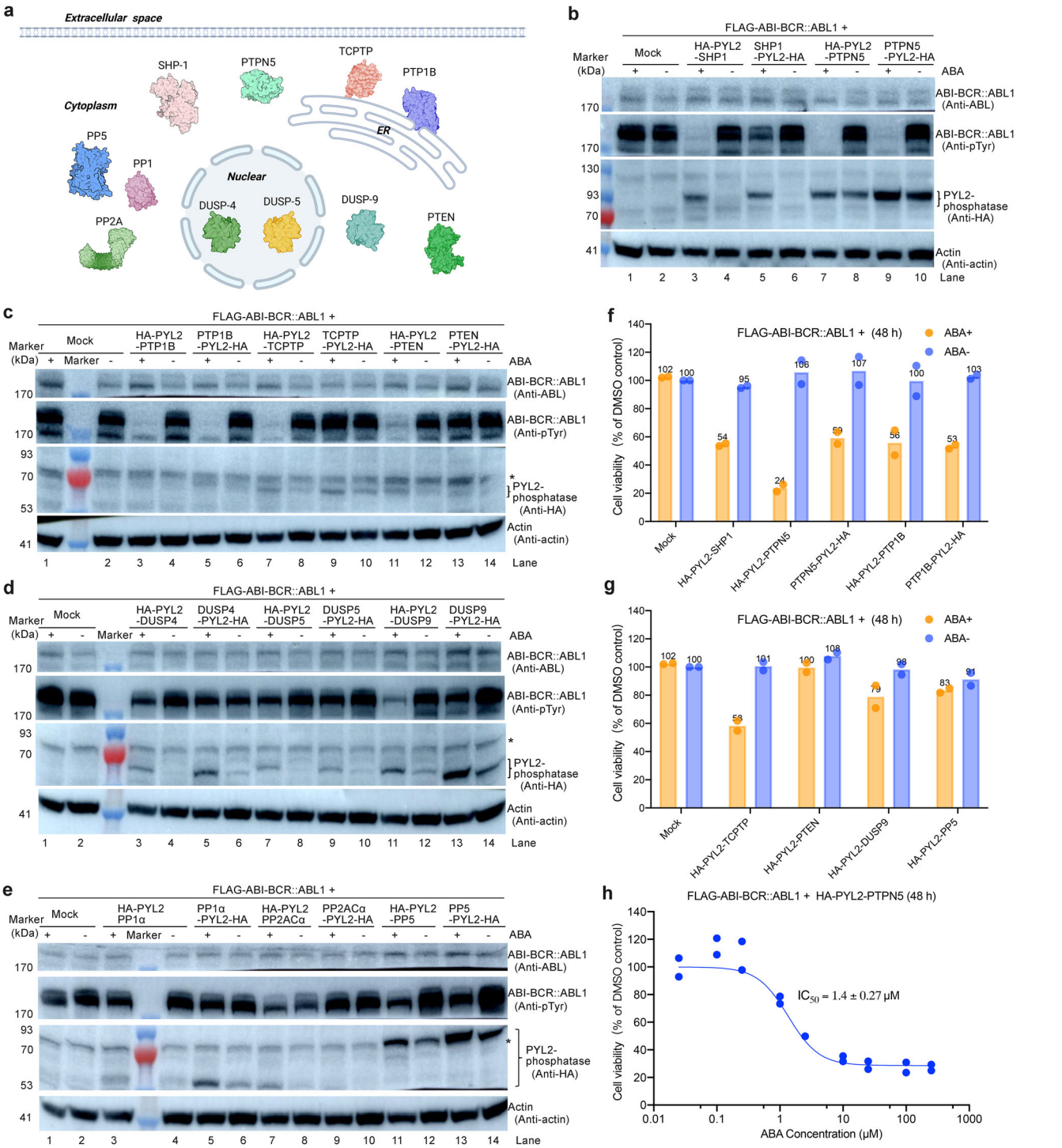

Fig. 2 | Identification of phosphatases that can dephosphorylate BCR::ABL1 when being recruited to BCR::ABL1. a Illustration of the subcellular localization of representative phosphatases in human cells. Created with BioRender.com. **b**–**e** Screening of phosphatases that can be recruited to BCR::ABL1 to regulate BCR::ABL1 phosphorylation in Ba/F3 cells using the ABA induced proximity system. The asterisk (*) indicates a non-specific band detected by the anti-HA antibody. **f**, **g** Inhibition of the viability of Ba/F3 cells expressing FLAG-tagged ABI-BCR::ABL1 by recruitment of different phosphatases to ABI-BCR::ABL1 using ABA. The cell viability of each group was normalized to that of the ABA-untreated mock group. The values represent the mean of two independent measurements with technical duplicates. **h** ABA inhibited the viability of Ba/F3 cells expressing FLAG-tagged ABI-BCR::ABL1 and HA-tagged PYL2-PTPN5, with an IC_{50} of 1.4 μM. The values represent the mean of two independent measurements with technical duplicates.

Synergism between ABA and the BCR::ABL1 inhibitor imatinib (IMA)

In line with the inhibitory effect of ABA on the proliferation of Ba/F3 cells, ABA reduced the pTyr level of BCR::ABL1 in a dose-dependent manner (Fig. 3a). We compared the activities of ABA with IMA. IMA inhibited ABI-BCR::ABL1 phosphorylation regardless of the presence of PYL2-PTPN5. In contrast, the activity of ABA was dependent on the presence of PYL2-PTPN5 (Fig. 3b).

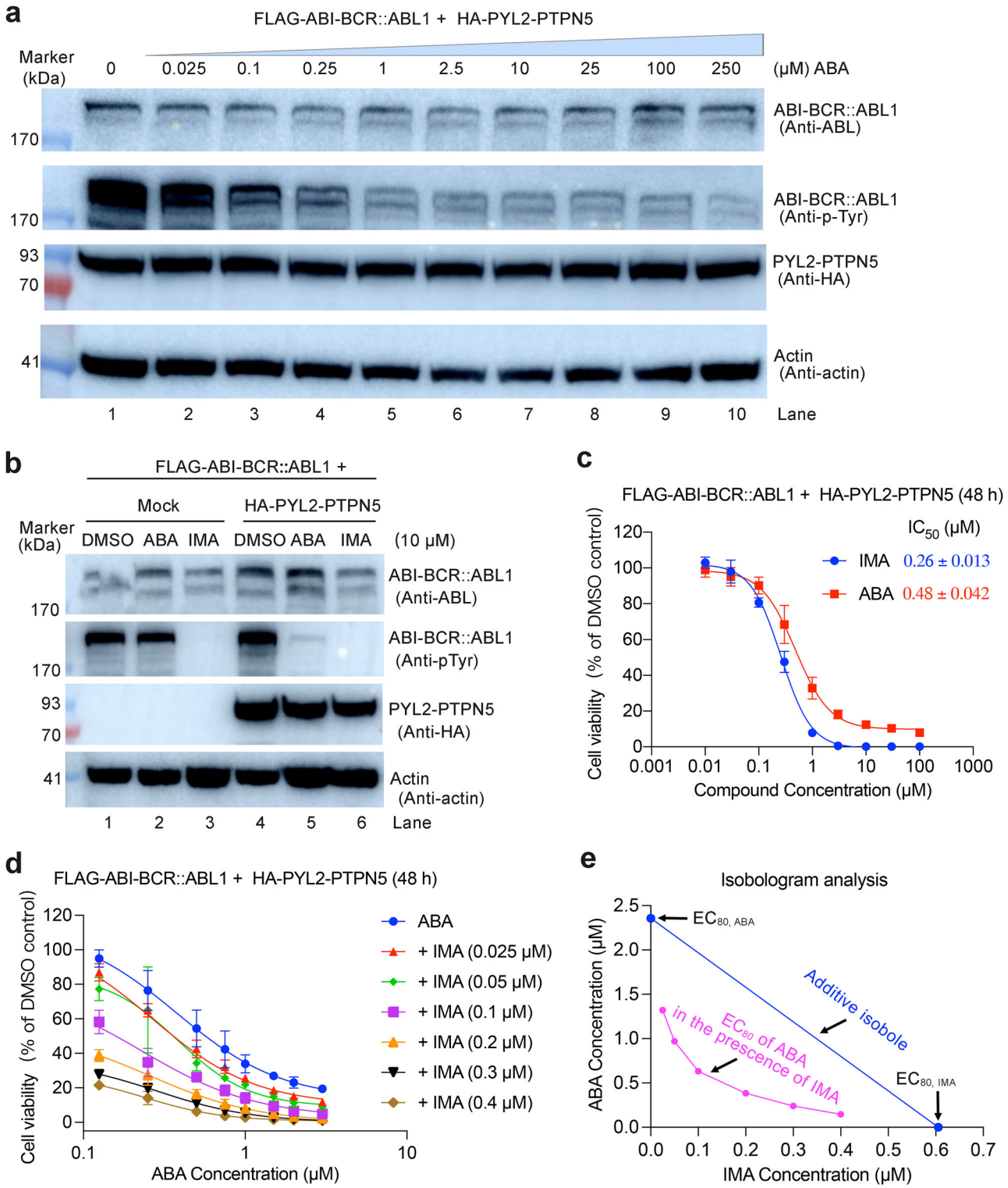

Fig. 3 | Regulation of the pTyr level of BCR::ABL1 in Ba/F3 cells using ABA and imatinib (IMA). a Dose-dependent effect of ABA on the pTyr level of BCR::ABL1 in Ba/F3 cells expressing FLAG-tagged ABI-BCR::ABL1 and HA-tagged PYL2-PTPN5. **b** Effects of IMA and ABA (10 μM) on the pTyr level of BCR::ABL1 in Ba/F3 cells expressing FLAG-tagged ABI-BCR::ABL1 alone or together with HA-tagged PYL2-PTPN5. **c**, **d** Inhibition of the proliferation of Ba/F3 cells expressing FLAG-tagged ABI-BCR::ABL1 and HA-tagged PYL2-PTPN5 by IMA or ABA alone (, or combinations of different concentrations of ABA and IMA (**d**). The data represent the mean ± SD of three independent measurements with technical duplicates. **e** Isobologram analysis reveals synergism between ABA-induced dephosphorylation and inhibition of the kinase activity of BCR::ABL1 by IMA. The line called additive isobole was plotted using the equation "$x/EC_{80,IMA} + y/EC_{80,ABA} = 1$", where "x" and "y" represent the concentrations of IMA and ABA, respectively, used in the combination treatment, while "$EC_{80,IMA}$" and "$EC_{80,ABA}$" represent the EC_{80} values of IMA and ABA, respectively, when they were used alone (**c**). The EC_{80} values of ABA in the presence of different concentrations of IMA (panel D) were calculated and used to plot the EC_{80} curve.

To test whether ABA-induced dephosphorylation has a synergistic effect with direct inhibition of the kinase activity of BCR::ABL1 by IMA, we treated the Ba/F3 cells expressing FLAG-tagged ABI-BCR::ABL and HA-tagged PYL2-PTPN5 with either ABA or IMA alone (Fig. 3c), as well as with combinations of different concentrations of ABA and IMA (Fig. 3d). We then conducted isobologram analysis[34], to evaluate the presence of synergism (Fig. 3e). The EC_{80} curve of ABA in the presence of different concentrations of IMA is below the additive isobole, indicating synergism between ABA and IMA.

BRAF(V600E) is sensitive to ABA induced dephosphorylation

Having found that recruitment of phosphatases to BCR::ABL1 dephosphorylated BCR::ABL1, we next tested using the ABA induced proximity system to control serine/threonine kinases. We focused on the RAF-MEK-ERK kinase signaling pathway that plays a pivotal role in the regulation of cell growth, differentiation, and survival[35]. Aberrant activation of this pathway contributes to the initiation and progression of many cancers[36]. Among the RAF kinases, BRAF carries the most prevalent oncogenic RAF mutation—BRAF V600E, which has been found in approximately 8% of human tumors, particularly in melanoma, colorectal, thyroid cancers[37,38]. We tried to regulate the kinase activity of the BRAF(V600E) mutant using three serine/threonine phosphatases, including PP1α, PP2ACα and PP5. PP1α and PP2ACα are the catalytic subunits of PP1 and PP2A, respectively. Previous studies have shown that the PP1 and PP2A can positively regulate wild-type RAF kinases[39,40], while PP5 plays a negative role[41].

We fused the FLAG-tagged ABI to the C terminus of BRAF(V600E) and fused the HA-tagged PYL2 to the N or C termini of the phosphatases, then stably expressed them in Ba/F3 cells to make the cells dependent on the RAF-MEK-ERK pathway after IL-3 withdrawal. ABA-induced recruitment of HA-tagged PYL2-PP1α and PYL2-PP2ACα to FLAG-tagged BRAF(V600E)-ABI was confirmed by purifying the kinase-phosphatase complexes using immobilized anti-FLAG antibody and subsequently conducting mass spectrometry (MS) analysis (Supplementary Table 1). In addition to PP1α and PP2ACα, several other subunits of PP1 and PP2A were also co-purified with FLAG-tagged BRAF(V600E)-ABI in the presence of ABA (Supplementary Table 1).

PP1α, PP2ACα and PP5 showed distinct effects on the BRAF(V600E)-MEK-ERK signaling pathway (Fig. 4a). Recruitment of PP1α did not have an apparent effect on the phosphorylation of S729 and S446 of BRAF, nor on the phosphorylation of S218/S222 of MEK, but increased the phosphorylation level of T202/Y204 of ERK (Fig. 4a, lanes 3-6). Recruitment of PP2ACα had little effect on the phosphorylation level of BRAF, MEK or ERK (Fig. 4a, lanes 7-10). In contrast, recruitment of PP5 dephosphorylated BRAF(V600E) at S729 and S446, inhibiting the phosphorylation of MEK S218/S222 and ERK T202/Y204 (Fig. 4a, lanes 11-14). We further confirmed that the distinct effects of PP1α and PP5 on ERK phosphorylation were attributed to the phosphatase activities of PP1α and PP5 by introducing catalytic-dead mutations H248K and H304A into PP1α and PP5, respectively (Fig. 4b, c). Recruitment of PP5 to BRAF(V600E) significantly inhibited the viability of the Ba/F3 cells (Fig. 4d). Similar results were observed when we fused the FLAG-tagged ABI to the N terminus of BRAF(V600E) (Supplementary Fig. 5). These results demonstrate that PP1α and PP5 have opposite effects on the RAF-MEK-ERK signaling pathway when they are recruited to BRAF(V600E); in addition, recruitment of PP5 to BRAF(V600E) is a feasible strategy to inhibit BRAF(V600E) activity (Fig. 4e).

The different effects of PP1α and PP5 on BRAF(V600E) signaling pathway are consistent with their effects on wild-type RAF signaling pathway reported by previous studies, in which it was found that PP1 dephosphorylated CRAF at S259 (corresponding to S365 in BRAF) to promote CRAF activation[39,40], while PP5 dephosphorylated CRAF at S338 (corresponding to S446 in BRAF) to inhibit CRAF activity[41]. However, it has been reported that the oncogenic mutation V600E allows BRAF to bypass the regulation by phosphorylation/dephosphorylation[42–46]. To understand the effects of PP1α and PP5 on BRAF(V600E), we harvested the Ba/F3 cells with and without ABA treatment (Supplementary Fig. 6a), enriched the FLAG-tagged BRAF(V600E) using anti-FLAG beads and quantified its phosphorylation using mass spectrometry (MS). In Ba/F3 cells expressing both FLAG-ABI-BRAF(V600E) and HA-PYL2-PP5, the addition of ABA induced dephosphorylation of BRAF(V600E) at S319/S325, S365, S399/T401, and S729; dephosphorylation of these residues was also observed in Ba/F3 cells expressing both BRAF(V600E)-ABI-FLAG and PP5-PYL2-HA, but to a less extent (Supplementary Fig. 6b–g). In Ba/F3 cells expressing both FLAG-ABI-BRAF(V600E) and HA-PYL2-PP1α, adding ABA decreased the phosphorylation at S365, S399/T401, and S729, but the decrease was not as significant as that in the presence of HA-PYL2-PP5 and ABA (Supplementary Fig. 6d, e, g).

Drug-resistant variants of BRAF(V600E) can be inhibited by recruiting PP5

Three BRAF inhibitors, including vemurafenib (VEM), dabrafenib, and encorafenib, have received approval for the treatment of cancers, such as melanomas and non-small cell lung cancers (NSCLC), that carry the BRAF V600E or V600K mutation[47]. Vemurafenib was approved for the treatment of BRAF-mutated melanomas in 2011 in the United States[48], but soon drug-resistant variants of BRAF(V600E) were identified[49]. Melanoma cell line SKMEL-239 carrying aberrant splicing variants of BRAF(V600E) lack the RAS binding domain showed strong resistance to VEM (Fig. 5a)[49]. Aberrant spliced BRAF(V600E) also exhibited resistance to dabrafenib and encorafenib[50,51]. We confirmed that in Ba/F3 cells co-expressing these spliced BRAF(V600E) and PP5 were resistant to VEM (Fig. 5b, c). The IC_{50} value of VEM against the full-length BRAF(V600E) was 0.4 μM but increased to around 30 μM against the p61 and p55 variants (Fig. 5b). In contrast, aberrant splicing of BRAF(V600E) did not confer resistance to ABA-induced dephosphorylation (Fig. 5d, e). These results demonstrate the potential of the induced dephosphorylation strategy in overcoming drug resistance caused by alterations of the kinases.

Recruitment of PP5 to MEK1 can inactivate MEK1

The dual-specificity kinases MEK1 and MEK2 are at the center of the RAF-MEK-ERK signaling pathway[52]. Human MEK1 shares a sequence identity of 80% with MEK2. The functions of MEK1 and MEK2 are redundant[53]. Therefore, we only focused on MEK1. We tested whether the ABA induced proximity system can regulate MEK1 activity. We fused FLAG-tagged ABI to the C terminus of MEK1, fused HA-tagged PYL2 to the N or C termini of PP1α, PP2ACα and PP5, then stably expressed them in Ba/F3 cells stably expressing BRAF(V600E). In the presence of ABA, HA-tagged PYL2-PP1α, PYL2-PP2ACα, and several other subunits of PP1 and PP2A were co-purified with FLAG-tagged MEK-ABI (Supplementary Table 1), indicating that ABA can promote the kinase-phosphatase interactions. Upon treatment with ABA, only in cells expressing HA-PYL2-PP5 we observed the decrease of both MEK-ABI phosphorylation and ERK phosphorylation (Fig. 6a). When the catalytic-dead mutation H304A was introduced into PP5, recruitment of HA-PYL2-PP5 could not decrease the phosphorylation level of either MEK or ERK (Fig. 6b). These results demonstrate that MEK1 can be inactivated by recruiting PP5 to it, and the phosphatase activity of PP5 is required (Fig. 6c).

Recruitment of PP5 to BRAF(V600E) cannot facilitate MEK1 dephosphorylation

Since MEK1 can form complex with BRAF[54,55], we wonder whether recruitment of PP5 to BRAF(V600E) can directly dephosphorylate MEK1. To answer this question, we used purified proteins to reconstitute an in vitro assay (Fig. 7a). Firstly, BRAF(V600E) with ABI fused to its C terminus was mixed with MEK1 in a kinase reaction buffer at 30 °C for 30 minutes to enable the phosphorylation of MEK1 at S218/S222 (Fig. 7b, lanes 1, 2, and 8). Secondly, PP5-PYL2-FLAG in buffers containing palmitoyl-CoA and $MnCl_2$ was added and incubated at 30 °C for 50 minutes to catalyze the dephosphorylation of BRAF and MEK1 (Fig. 7b, lanes 3 and 9). PP5 alone is in an auto-inhibited state and palmitoyl-CoA was used as an activator of

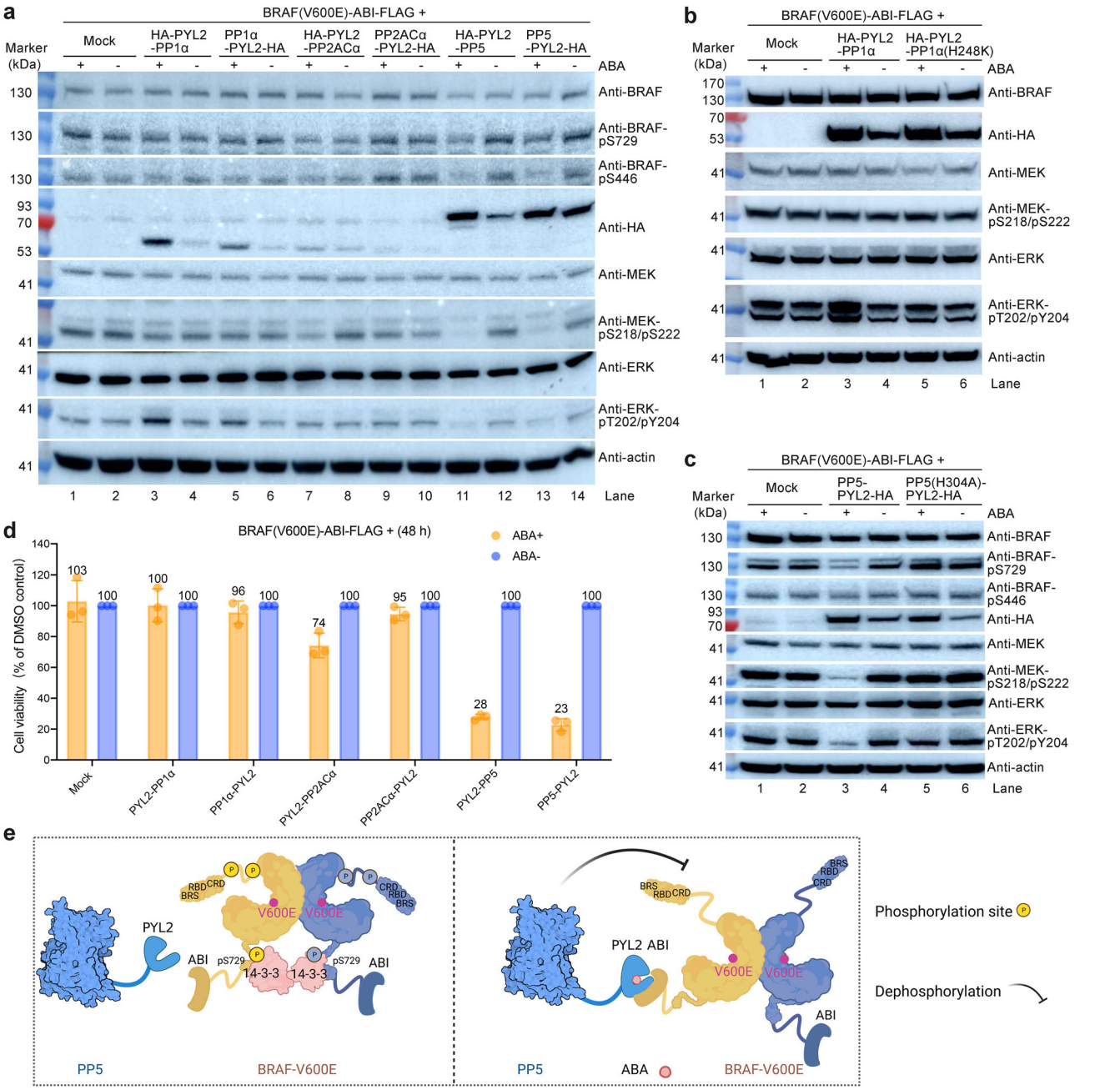

Fig. 4 | Regulation of BRAF(V600E) activity by recruiting protein serine/threonine phosphatases. a Recruitment of PP1α, PP2ACα and PP5 to BRAF(V600E) using the ABA induced proximity system in Ba/F3 cells showed distinct effects on the BRAF(V600E)-MEK-ERK signaling pathway. **b** Recruitment of wild-type PP1α but not the catalytic-dead mutant PP1α(H248K) to BRAF(V600E) in Ba/F3 cells increased the phosphorylation level of ERK. **c** Recruitment of wild-type PP5 but not the catalytic-dead mutant PP5(H304A) to BRAF(V600E) in Ba/F3 cells blocked the activation of MEK and ERK. **d** Inhibition of the viability of Ba/F3 cells expressing BRAF(V600E)-ABI-FLAG by recruitment of PP1α, PP2ACα or PP5 to BRAF(V600E). The viability of the ABA-treated cells was normalized to that of the untreated cells. The values represent the mean ± SD of three independent measurements with technical duplicates. **e** Illustration of the regulation of BRAF(V600E) by PP5 using the ABA induced proximity system. Created with BioRender.com.

PP5[56]. $MnCl_2$ was added because the catalytic activity of PP5 requires the presence of two metal ions, usually Mn^{2+}, at its catalytic center[57,58]. In previous studies, 500 μM or even higher concentrations of $MnCl_2$ was used to support the activity of purified PP5 in in vitro assays[56,58]. However, the cellular concentration of free Mn^{2+} ions is at a low micromolar level[59]. Therefore, we tested two concentrations of $MnCl_2$ in the reaction: 50 μM and 500 μM. Thirdly, the reactions were treated with ABA, dabrafenib (DAB, an inhibitor of BRAF), ABA together with DAB, or the same volume of DMSO and incubated at 30 °C for additional 50 minutes (Fig. 7b, lanes 4-7 and 10-13). The assay was repeated five times and the phosphorylation of BRAF(V600E) at S729 and that of MEK1 at S218/S222 were quantified by western blotting and normalized to the level of BRAF(V600E) or MEK1 (Fig. 7c, d).

In the presence of 50 μM $MnCl_2$, the phosphorylation of BRAF(V600E) at S729 was slightly decreased upon adding PP5 but the decrease was not statistically significant regardless of whether ABA or Dabrafenib was added or not (Fig. 7c, left panel); the phosphorylation of MEK1 at S218/S222 was also slightly decreased upon adding PP5 and the decrease was also not statistically significant, but upon treatment with Dabrafenib, the phosphorylation of MEK1 at S218/S222 was decreased by

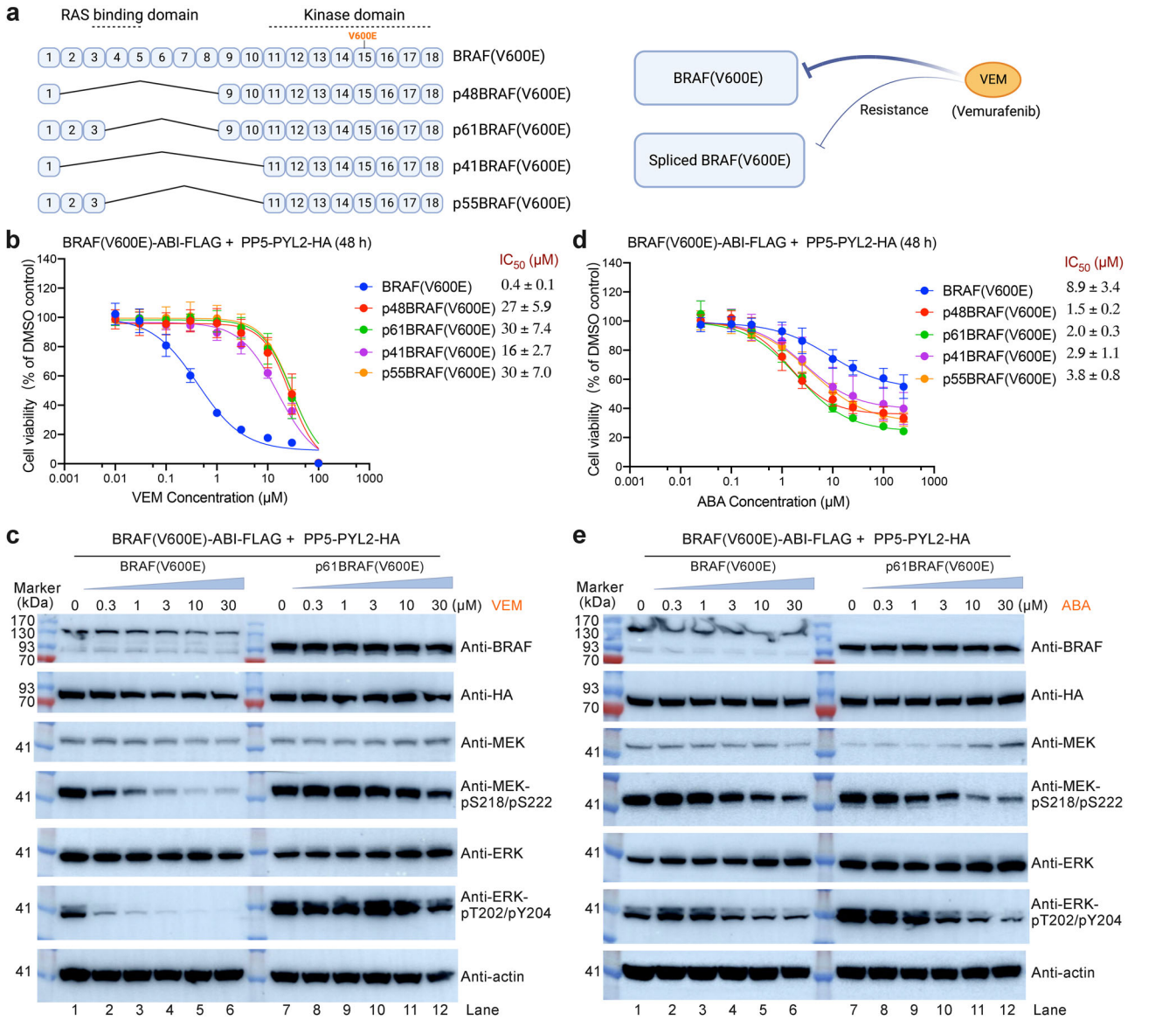

Fig. 5 | Splicing variants of BRAF(V600E) resistant to vemurafenib (VEM) are sensitive to ABA-induced dephosphorylation. a Illustration of the exon organization of the aberrant splicing variants of BRAF(V600E) that are resistant to vemurafenib (VEM). Created with BioRender.com. **b, d** Ba/F3 cells expressing full-length or aberrantly spliced BRAF(V600E)-ABL-FLAG together with PP5-PYL2-HA were treated with VEM (**b**) or ABA (**d**), and the cell viability was measured after 48 h. The data represents the mean ± SD of four independent measurements, each with technical duplicates. **c, e** Effects of VEM (**c**) and ABA (**e**) on the phosphorylation levels of MEK and ERK in Ba/F3 cells expressing BRAF(V600E)-ABI-FLAG or p61BRAF(V600E)-ABI-FLAG together with PP5-PYL2-HA.

40% (Fig. 7c, right panel). In contrast, in the presence of 500 μM $MnCl_2$, the phosphorylation of BRAF(V600E) at S729 was significantly decreased after adding PP5 and further decreased upon treatment with ABA (Fig. 7d, left panel); the phosphorylation of MEK1 at S218/S222 was not changed after adding PP5 (Fig. 7d, right panel).

These results indicate that the recruitment of PP5 to BRAF(V600E) promoted the dephosphorylation of BRAF(V600E), but did not facilitate MEK1 dephosphorylation. Additionally, the phosphatase activity of PP5 is controlled by $MnCl_2$ concentration. PP5 dephosphorylated MEK1 at low $MnCl_2$ concentration (50 μM), while at high $MnCl_2$ concentration (500 μM), PP5 recognized BRAF(V600E) but not MEK1 as its substrate. However, the implication of this finding for the function of PP5 in a cellular context has yet to be studied.

Discussion

Using the tyrosine kinase BCR::ABL1 and the serine/threonine kinases BRAF(V600E) and MEK1 as examples, we have shown that the ABA induced proximity system provided a convenient method to reversibly control kinase activities and to identify phosphatases that can be recruited to inhibit the kinases. When fusing the ABI and PYL tags to kinases and phosphatases, the positions to which the tags are fused, as well as the length and flexibility of the linkers between ABI and the kinases, and between PYL and the phosphatases, should be taken into consideration. This can help minimize the effect of the tags on the enzymatic activities of the kinases and phosphatases, and can also induce the optimal proximity between the phosphorylation sites of the kinases and related phosphatases, promoting efficient dephosphorylation reactions.

Though the ABA induced proximity system has been studied extensively, the effect of ABA on the stability of PYL2 has not been reported. We have shown that binding of ABA to PYL2 significantly increased the cellular concentration of PYL2. Additionally, when PYL2 was fused to phosphatases such as SHP1 and PP1α, the cellular concentrations of the fusion proteins were also increased significantly upon adding ABA. This unexpected finding suggests that ABA not only induces the proximity of kinases and

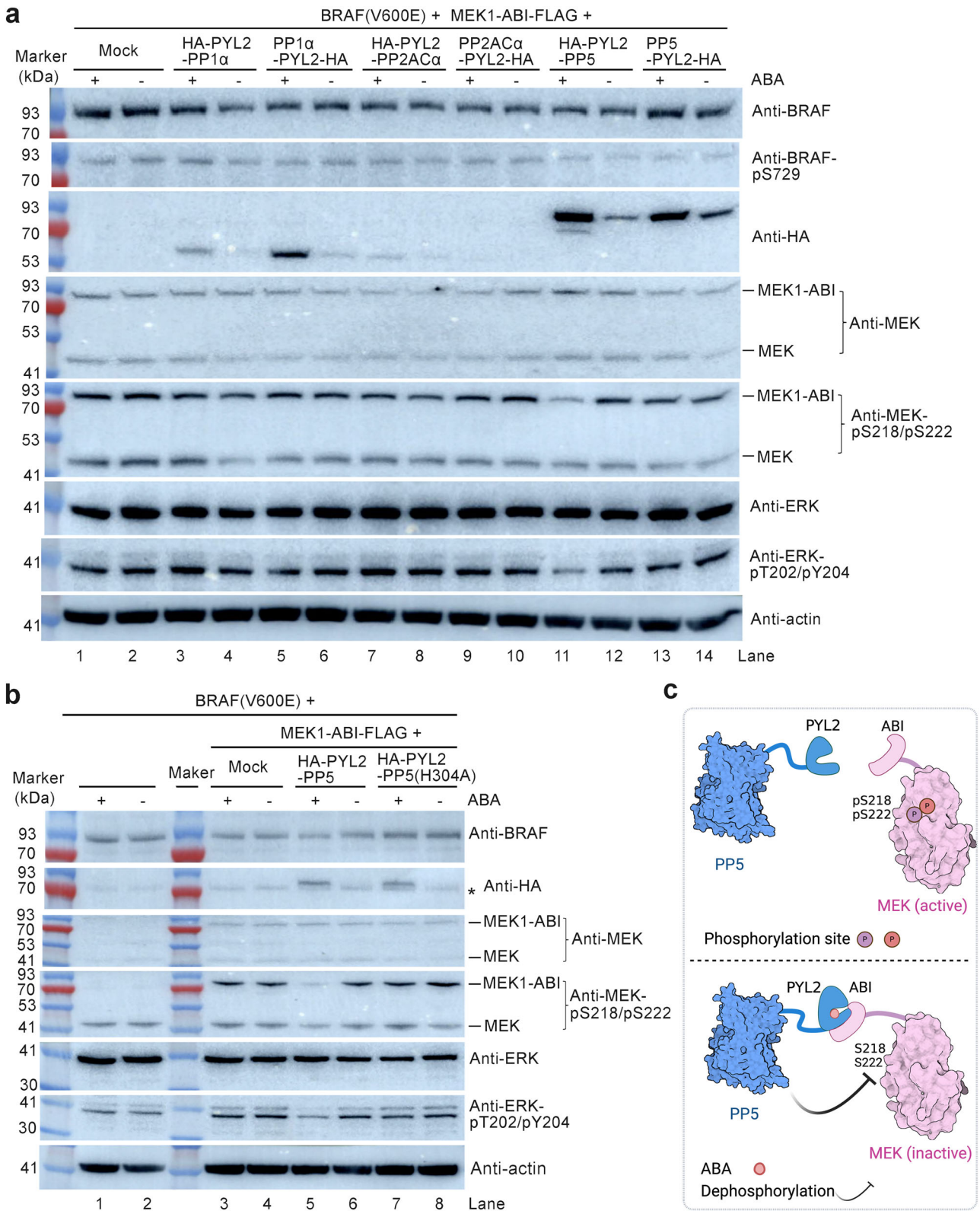

Fig. 6 | Regulation of MEK1 activity by recruiting protein serine/threonine phosphatases. a Effects of PP1α, PP2ACα and PP5 on MEK1 activity when they were recruited to MEK1 in Ba/F3 cells expressing BRAF(V600E) using the ABA induced proximity system. **b** Recruitment of wild-type PP5 but not the catalytic-dead mutant PP5(H304A) to MEK1 in Ba/F3 cells expressing BRAF(V600E) decreased MEK1 at S218/S222 and inhibited the activation of ERK. The asterisk (*) indicates a non-specific band detected by the anti-HA antibody. **c** Illustration of the regulation of MEK by PP5 using the ABA induced proximity system. Created with BioRender.com.

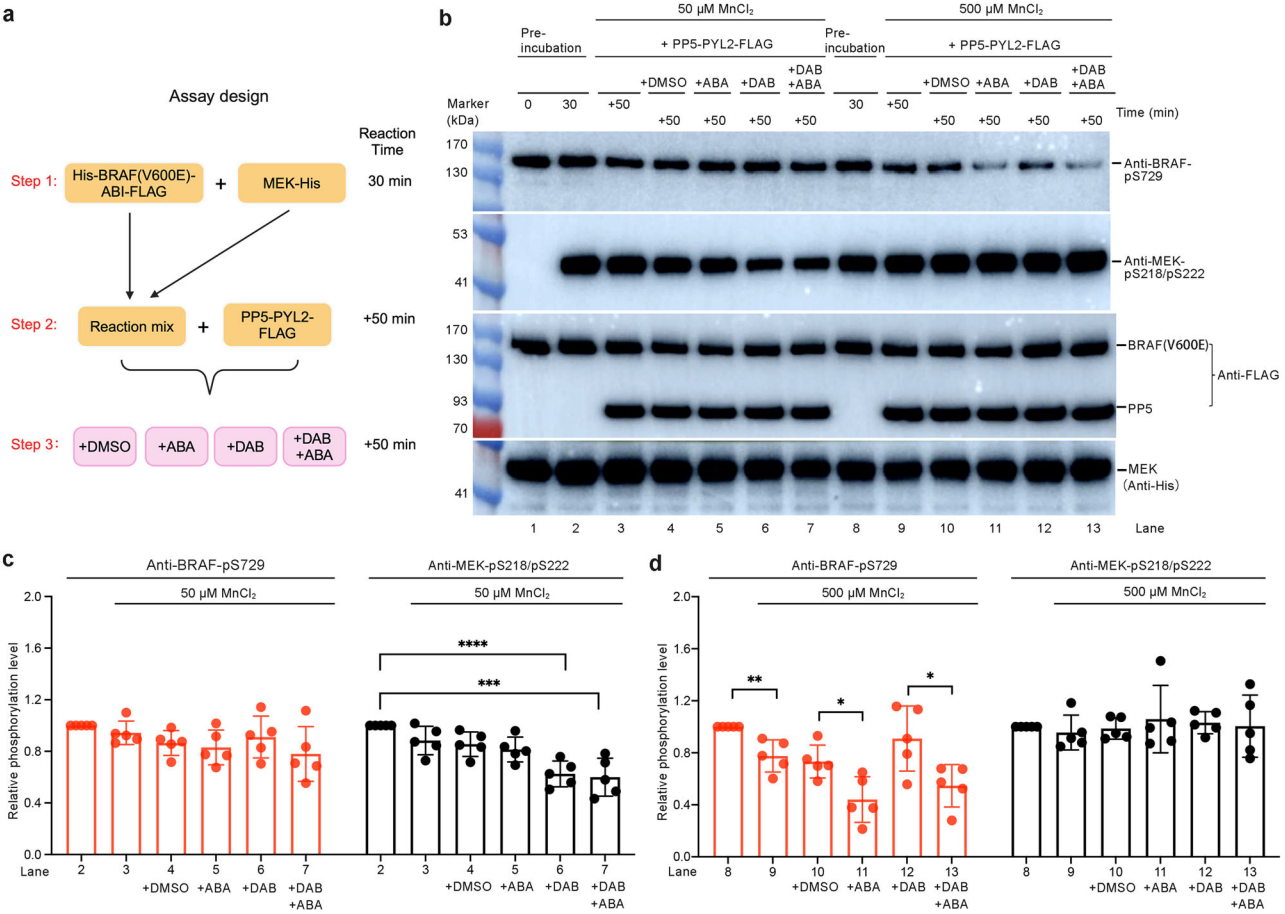

Fig. 7 | Dephosphorylation of BRAF(V600E) and MEK1 by PP5 can be regulated by Mn^{2+} concentration. a Schematic of the assay design. In step 1, purified BRAF(V600E)-ABI with His tag at its N terminus and FLAG tag at its C terminus was first incubated with purified His-tagged MEK1 in a kinase reaction buffer at 30°C for 30 minutes; in step 2, purified FLAG-tagged PP5-PYL2 was added and incubated for additional 50 minutes in the presence of 50 or 500 μM $MnCl_2$; in the step 3, ABA, the BRAF inhibitor Dabrafenib (DAB), ABA plus DAB, or the same volume of DMSO was added and incubated for additional 50 minutes. **b** Analysis of the effects of Mn^{2+} concentration, ABA, and DAB on the activity of PP5 to dephosphorylate BRAF and MEK1 by using western blot. **c, d** Phosphorylation of BRAF(V600E) at S729 and that of MEK1 at S218/S222 were quantified and normalized with their protein bands. Then the normalized phosphorylation signals were further normalized with the phosphorylation signals in lane 2 (50 μM $MnCl_2$) or normalized with that in lane 8 (500 μM $MnCl_2$). The data represent the mean ± SD of five independent measurements and were analyzed using the unpaired *t*-test in Prism to calculate the two-tailed *P* values: ****$P < 0.0001$; ***$P < 0.001$; **$P < 0.01$; *$P < 0.05$.

phosphatases, but also increases the concentrations of phosphatases. Accordingly, we propose that the PYL2-ABA pair can be used to regulate protein concentration in mammalian cells. Since we demonstrated that the protein levels of both FLAG-ABI-BCR::ABL1 and HA-PYL2-SHP1 in the Ba/F3 cells were decreased upon MG132 treatment, and ABA treatment partially restored the protein levels (Supplementary Fig. 3e), it would be interesting to figure out how the protein levels of FLAG-ABI-BCR::ABL1 and HA-PYL2-SHP1 are regulated by MG132 and ABA.

Using the ABA-induced proximity system, we found that BCR::ABL1, the well-known drug target for CML therapy, can be inhibited by the recruitment of several cytoplasmic phosphatases. Additionally, we showed that ABA exhibits a synergistic effect in combination with the BCR::ABL1 inhibitor IMA, emphasizing the importance of developing bifunctional molecules capable of recruiting endogenous cytoplasmic phosphatases to BCR::ABL1 for the treatment of CML.

Another important finding is that the oncogenic kinase BRAF(V600E) and its drug-resistant splicing variants can still be controlled by phosphorylation and dephosphorylation through ABA-induced recruitment of phosphatases. Previous studies have suggested that the oncogenic mutation V600E enables BRAF to bypass the phosphorylation regulation[42–46]. Though phosphorylation can still affect the kinase activity and heterodimerization of BRAF(V600E) with CRAF, it has been reported that phosphorylation has little effect on the transforming activity of BRAF(V600E)[44,60]. In addition, alanine mutations in the phosphorylation sites on the activation loop showed minimal impact on the signaling potential of the BRAF V600F and V600E mutants[46,61]. But we showed that the BRAF(V600E) mediated ERK phosphorylation was downregulated by PP5 but slightly upregulated by PP1α. The phosphatase activities of PP1α and PP5 are necessary for their distinct effects on ERK phosphorylation (Fig. 4b, c). Recruitment of PP5 to BRAF(V600E) dephosphorylated BRAF(V600E) at multiple Ser/Thr sites. Dephosphorylation of BRAF(V600E) at these sites, except S319/S325, was also observed by Oberoi et al. when they treated the HSP90–CDC37–BRAF(V600E) complex with PP5 and quantified the phosphorylation using mass spectrometry[62]. Phosphorylation of BRAF at S365 and T401 has been reported to negatively regulate wild-type BRAF, while phosphorylation at S729 positively regulate wild-type BRAF[44,45]. It has also been reported that mutation of S365 to alanine, mimicking the dephosphorylation state of S365, increased homodimerization of BRAF(V600E) to promote downstream signaling[63]. Therefore, both PP1α and PP5 may have positive and negative effects on the activity of BRAF(V600E) when they are recruited to it. In addition, since BRAF has been reported to form complexes with numerous proteins[9,64], the distinct effects of PP1α and PP5 on BRAF(V600E) may also be attributed to

dephosphorylation of proteins that interact with BRAF(V600E). Further studies are required to unveil the links between the phosphatase activities of PP1α and PP5 and the phosphorylation of ERK.

In addition to the observation that recruitment of PP5 to BRAF(V600E) effectively inhibited the proliferation of Ba/F3 cells expressing BRAF(V600E) or the drug-resistant splicing variants of BRAF(V600E), we have shown that recruitment of PP5 to MEK1 dephosphorylated and inhibited MEK1. The kinase activities of MEK kinases (MEK1 and MEK2) are tightly controlled by phosphorylation. Our results suggest that PP5 can be used to regulate MEK phosphorylation. Development of bifunctional molecules to recruit endogenous PP5 to MEK or RAF kinases is a promising strategy for cancer treatment.

Methods

Cell culture

The Ba/F3 cells (from Chinese National Cell Bank, Beijing, China) were cultured in RPMI medium (Hyclone, Cat# SH30809.01) supplemented with 10% FBS (Gibco, Cat# 10270-106), 1% penicillin-streptomycin solution (Hyclone, Cat# SV30010) and 10 ng/mL recombinant mouse IL-3 (GenScript, Cat# Z03111). The 293 T cells were cultured in high-glucose DMEM (Hyclone, Cat# C11995500BT) supplemented with 10% FBS and 1% penicillin-streptomycin solution. After cryorecovery, the cells were cultured in a humidified incubator with 5% CO_2 at 37 °C for at least two generations before they were used in the assays. The 293 F cells were cultured in SMM293-TII medium (Sino Biological, Cat# M293TII) supplemented with 1% penicillin-streptomycin solution at 37 °C under 5% CO_2 in a Multitron-Pro shaker (Infors, 110 rpm). All cell lines were tested mycoplasma negative using mycoplasma detection kit (Beyotime).

Genes and cloning

To build the ABA induced proximity system, we used the *Arabidopsis thaliana* ABI1 (accession number in PubMed: NP_194338.1) and PYL2 (accession number in PubMed: NP_180174.1). Specifically, we used a truncated ABI1 containing residues V126 to L422 with the D143A mutation and called it ABI, and used a truncated PYL2 containing residues T11 to D188 and called it PYL2 in this study.

FLAG-tagged ABI was fused to the N or C termini of kinases including BCR::ABL1 (Addgene plasmid #38158), BRAF (accession number in PubMed: NP_004324.2) with the V600E mutation, aberrantly spliced BRAF(V600E), and MEK1 (accession number in PubMed: NP_002746.1) to obtain the following constructs: FLAG-ABI-BCR::ABL1, FLAG-ABI-BARF(V600E), BRAF(V600E)-ABI-FLAG, spliced BRAF(V600E)-ABI-FLAG, and MEK1-ABI-FLAG. BCR::ABL1 alone, and FLAG-ABI were used as controls. In these constructs, there was a GS linker between the FLAG tag (DYKDDDDK) and ABI, and a SGGGGS linker between ABI and the kinases. To generate retroviruses, the coding sequences of these constructs were separately cloned into MSCV-PGK-puroR vector (Addgene plasmid # 68469); the coding sequence of BRAF(V600E) was cloned into a MSCV-IRES-EGFP vector (Addgene plasmid # 20672).

HA-tagged PYL2 was fused to the N or C termini of phosphatases including SHP1 (accession number in PubMed: NP_002822.2), PTPN5 (accession number in PubMed: NP_008837.1), PTP1B (accession number in PubMed: NP_002818.1), TCPTP (accession number in PubMed: NP_002819.2), PTEN (accession number in PubMed: NP_000305.3), DUSP4 (accession number in PubMed: NP_001385.1), DUSP5 (accession number in PubMed: NP_004410.3), DUSP9 (accession number in PubMed: NP_001305432.1), PP1α (accession number in PubMed: NP_002699.1), PP2ACα (accession number in PubMed: NP_002706.1) and PP5 (accession number in PubMed: NP_006238.1)] to obtain the following constructs: HA-PLY2, HA-PLY2-SHP1, SHP1-PLY2-HA, HA-PLY2(K64A)-SHP1, HA-PLY2-SHP1(C453S), HA-PLY2-PTPN5, HA-PLY2-PTPN5(C496S), PTPN5-PLY2-HA, HA-PLY2-PTP1B, HA-PLY2-PTP1B(C215S), PTP1B-PLY2-HA, HA-PLY2-TCPTP, HA-PLY2-TCPTP(C216S), TCPTP-PLY2-HA, HA-PLY2-PTEN, HA-PLY2-PTEN(C124S), PTEN-PLY2-HA, HA-PLY2-DUSP4, DUSP4-PLY2-HA, HA-PLY2-DUSP5, DUSP5-PLY2-HA, HA-PLY2-DUSP9, DUSP9-PLY2-HA, HA-PLY2-PP1α, HA-PLY2-PP1α(H248K), PP1α-PLY2-HA, HA-PLY2-PP2ACα, PP2ACα-PLY2-HA, HA-PLY2-PP5, PP5-PLY2-HA, HA-PLY2-PP5(H304A), and PP5(H304A)-PLY2-HA. In these constructs, there was a GSG linker between the HA tag (YPYDVPDYA) and PYL2, and a SGGGGSG linker between PYL2 and the phosphatases. To generate retroviruses, the coding sequences of these constructs were separately cloned into a MSCV-PGK-neoR vector.

To construct plasmids for recombinant protein expression, the coding sequences of FLAG-ABI-BCR::ABL1, BRAF(V600E)-ABI-FLAG with an 8x His-tag at its N terminus, and PP5-PYL2-FLAG were separately cloned into the multiple cloning site of a pcDNA3.1 vector. The coding sequence of PYL2-SHP1 with a 6x His-tag at its N terminus was cloned into the multiple cloning site of a modified pET15b vector. The coding sequence of full-length human MEK1 without stop codon was cloned into a pET21b vector.

Preparation of mouse stem cell virus (MSCV)

10 mL of the 293 T cells (3x 10^5 cells/mL) were plated in a 10-cm dish. Once the cells were grown to 60% confluency, they were transfected with 7 μg of pCL-Eco (Addgene plasmid # 12371) and 13 μg of MSCV plasmids using 40 μg of Linear Polyethylenimine 25,000 (Polysciences, Cat# 23966) following the manufacturer's instructions (Takara Bio). The medium was exchanged 8 h after transfection. The cells were cultured for 48 h after transfection, then the supernatant was harvested and filtered through a 0.22 μm syringe filter. The filtrate containing the MSCV retrovirus was used immediately or stored at -80 °C.

Generation of stably transduced Ba/F3 cells

To generate Ba/F3 cells stably transduced with MSCV retrovirus carrying the coding sequence of FLAG-ABI, FLAG-ABI-BCR::ABL1, BCR::ABL1, FLAG-ABI-BARF(V600E), BRAF(V600E)-ABI-FLAG, or spliced BRAF(V600E)-ABI-FLAG, 1x 10^6 Ba/F3 cells per well in 1 mL of RMPI medium containing 20% FBS, 20 ng of mouse IL-3 and 10 μg of polybrene (Merck, Cat# TR-1003-G) were plated into 6-well plates (Corning, Cat# 3516), then 1 mL per well of the retrovirus was added. The Ba/F3 cells were spinfected by centrifugation at 1,000 g for 90 min at 32 °C following the manufacturer's instructions (Takara Bio) and then cultured overnight, followed by replacing the medium with fresh RPMI complete medium (RPMI medium, 10% FBS, 1% P/S) supplied with 10 ng /mL mouse IL-3. 48 h after transduction, the medium was replaced by the RPMI selection medium (RPMI medium, 10% FBS, 1% P/S and 2 μg/mL puromycin) with 10 ng/mL mouse IL-3. The cells were maintained under puromycin (invivogen, Cat# ant-pr) selection for 7 days, passaging as required. Then the transduced cells, except that transduced with FLAG-ABI retrovirus, were cultured in RPMI complete medium without IL-3 to make the cells dependent on the kinase activity of BCR::ABL1 or BRAF(V600E).

To generate Ba/F3 cells stably transduced with BRAF(V600E) retrovirus, 1x 10^6 Ba/F3 cells per well in 1 mL of RMPI medium containing 20% FBS, 20 ng of mouse IL-3 and 10 μg of polybrene were plated into 6-well plates, then 1 mL per well of the retrovirus was added. The Ba/F3 cells were spinfected by centrifugation at 1,000 g for 90 min at 32 °C following the manufacturer's instructions (Takara Bio) and then cultured overnight, followed by replacing the medium with fresh RPMI complete medium (RPMI medium, 10% FBS, 1% P/S) supplied with 10 ng /mL mouse IL-3. 48 h after transduction, the cells were sorted using FACS (MA900, Sony) based on the EGFP expression. The cells were cultured in RPMI complete medium supplemented with IL-3 for 5 days. The cells were then spun down, washed once with DPBS and resuspended in RPMI complete medium without IL-3 to make the cells dependent on the kinase activity of BRAF(V600E). The stably transduced cells were further transduced with MEK1-ABI-FLAG retrovirus following the same transduction protocol, except that the stably transduced cells were selected using puromycin instead of FACS, and cultured in the absence of IL-3.

The Ba/F3 cells stably transduced with retroviruses carrying FLAG-ABI or kinase coding sequences were further transduced with retroviruses

carrying phosphatase coding sequences following similar transduction protocols described above, and the stably transduced cells were selected by treatment with 800 μg/mL of G418 (invivogen, Cat# ant-gn-5) for 7 days. As for the mock groups, the retroviruses carrying empty MSCV vectors were used to transduce the Ba/F3 cells.

Immunoblotting assay

ABA (Cat# 862169-250MG) was prepared as a 250 mM stock in DMSO (Sigma, Cat# D2650-100mL). Imatinib (IMA) (Cat# T6230), MG132 (Cat# S2619), and vemurafenib (VEM) (Cat# T8654) were prepared as 100 mM stocks in DMSO. For stably transduced Ba/F3 cells, the cells (2x 10^6 cells/mL) were transferred to 6-well plates (1 mL/well), followed by adding 2 mL of RPMI complete medium per well supplemented with ABA, IMA, VEM, MG132, or DMSO. Unless otherwise noted, the final concentrations of ABA, IMA and MG132 were 250 μM, 1 μM, and 5 μM, respectively.

The cells were cultured for 12 h, then pelleted by centrifugation (1,000 g, 2 min). The pellet was washed with ice-cold PBS (1 mL x 2), then lysed in RIPA buffer supplemented with protease inhibitors and phosphatase inhibitors on ice for 20 min. The lysates were centrifuged at 22,000 g for 10 min, then the protein concentration in the supernatant was determined by BCA protein assay (Thermo Fisher Scientific, Cat# 23225 and Cat# 23227). The supernatants containing equal amount of total protein (20-40 μg) were mixed with 2x SDS loading buffer, heated at 95 °C for 5 min, subjected to 4-20% SDS-PAGE (GenScript, Cat# M00657) and transferred to 0.2 μm pore size PVDF membrane (Merck Millipore). The membrane was blocked with 5% non-fat milk (Beyotime, Cat# P0216-1500g) in TBST for 1 h at room temperature with shaking, then cut horizontally according to the molecular weight of target proteins, followed by incubation with primary antibodies for 1 h at room temperature or overnight at 4 °C with shaking. The membrane was then washed with TBST for 5 times, incubated with appropriate HRP-conjugated secondary antibodies (Merck Millipore, Cat# AP127P or Cat# AP156P) for 1 h at room temperature, and washed 5 times with TBST. The secondary antibodies on the PVDF membrane were visualized by adding ECL western blot reagents (FDbio, Cat# FD8020), followed by detection of the luminance signal using Amersham Imager 680.

Primary antibodies used in this study include Anti-actin (Immunoway, Cat# YM3028), Anti-FLAG (Sigma, Cat# F1804), Anti-HA (Abcam, Cat# ab9110), Anti-His (GenScript, Cat# A00186-100), Anti-c-ABL (Thermo Invitrogen™, Cat# MA5-14398), Anti-SHP1 (Abcam, Cat# ab131537), Anti-phospho-Tyr (CST, Cat# 9416S), Anti-STAT5 (CST, Cat# 94205S), Anti-phospho-STAT5 (Tyr694) (CST, Cat# 9359S), Anti-CrkL (Abcam, Cat# ab151791), Anti-phospho-CrkL (Tyr207) (CST, Cat# 3181S), Anti-AKT (CST, Cat# 4691S), Anti-phospho-AKT (Ser473) (CST, Cat# 4060 T), Anti-MEK1/2 (CST, Cat# 4694S), Anti-phospho-MEK1/2 (Ser217/221) (CST, Cat# 9154S), Anti-BRAF (CST, Cat# 14814S), Anti-phospho-BRAF (Ser445) (CST, Cat# 2696S), Anti-phospho-BRAF (Ser729) (Abcam, Cat# ab124794), Anti-phospho-BRAF (Thr401) (Abcam, Cat# ab68215), Anti-MAPK (ERK1/2) (CST, Cat# 4695S), Anti-phospho-MAPK (ERK1/2) (Thr202/Tyr204) (CST, Cat# 4370S). The Anti-phospho-MAPK (ERK1/2) (Thr202/Tyr204) antibody detects dually phosphorylated ERK1 (at Thr202 and Tyr204) and ERK2 (at Thr185 and Tyr187), and mono-phosphorylated ERK1 (at Thr202) and ERK2 (at Thr185).

Cell viability assay

80 μL per well of the transduced Ba/F3 cells (1x 10^4 cells) were seeded into 96-well white wall / clear bottom plates (Corning, Cat# 3610) and cultured overnight. Then 20 μL per well of serial dilutions of kinase inhibitors, ABA in RPMI complete medium was added. After additional 48 h, the cell viability was measured by using the CellTiter-Glo® luminescence-based assay (Promega, Cat# G7571). The viability was normalized to that in the DMSO control group. The data from 2 or 3 or 4 independent measurements with technical duplicates were analyzed in GraphPad Prism 7. To get the IC_{50} values, the data was fitted using the built-in nonlinear regression method "[Inhibitor] vs. response -- Variable slope (four parameters)".

Protein expression and purification

The FLAG-ABI-BCR::ABL1, His-BRAF(V600E)-ABI-FLAG and PP5-PYL2-FLAG were transiently expressed in 293 F cells and purified by Anti-FLAG Affinity Resin (GenScript, Cat# L00432-25). 1 L of 293 F cells at a density of 2x 10^6 cells/mL in SMM293-TII medium were transfected with 1-1.5 mg of the pcDNA3.1 plasmid and Linear Polyethylenimine 25,000 (mass DNA:mass PEI = 1:2). The transfected cells were cultured for 48 h, then harvested by centrifugation (Thermo Fisher SORVALL LYNX 6000 Centrifuge) at 4,000 g for 10 min at 4 °C. The cell pellets were resuspended in the lysis buffer (25 mM Tris 8.0, 150 mM NaCl, 5% glycerol) supplemented with 1.3 μg/mL Aprotinin (VWR, Cat# E429), 1 μg/mL Pepstain (VWR, Cat# J583), 5 μg/mL Leupeptin (VWR, Cat# J580) and 1 mM PMSF (Macklin, Cat# P6140), and lysed by ultrasonication (SONICS vibra cell™). The cell lysates were centrifuged at 22,000 g at 4 °C for 1 h (BECKMAN Avanti JXN-26 Centrifuge), then the target proteins in the supernatants were purified by using anti-FLAG affinity resin following the manufacturer's protocol. For FLAG-ABI-BCR::ABL1, it was further purified by a Source-15Q (GE Healthcare). The eluates from anti-FLAG affinity resin or Source-15Q column were supplemented with 5 mM Dithiothreitol (DTT) and further purified by Superdex 200 increase 10/300 GL column (GE Healthcare) and eluted by SEC buffer (25 mM HEPES 7.4, 150 mM NaCl). The peak fractions were pooled and concentrated for biochemical assays.

The His-PYL2-SHP1 and MEK-His were overexpressed in *Escherichia coli* BL21(DE3) and purified by TALON Metal Affinity Resin (TaKaRa, Cat# 635504). The plasmids were transformed into BL21(DE3) cells. The cells were cultured in LB medium supplemented with 0.1 mg/mL ampicillin at 37 °C until OD600 reached 1-1.5, then cooled to 20 °C followed by addition of 200 μM β-D-thiogalactopyranoside (IPTG). Then the cells were cultured at 20 °C overnight. The cells were harvested by centrifugation at 4,000 g for 10 min at 4 °C and resuspended in the lysis buffer (25 mM Tris 8.0, 150 mM NaCl, 5% glycerol) supplemented with 1 mM PMSF and lysed by ultrasonication. The cell lysates were centrifuged at 22,000 g at 4 °C for 1 h (BECKMAN Avanti JXN-26 Centrifuge), then the target proteins in the supernatants were purified by using TALON Metal Affinity Resin following the manufacturer's protocol. The eluates were supplemented with 5 mM Dithiothreitol (DTT) and loaded into a Source-15Q column (GE Healthcare) and eluted by a linear gradient from 100% buffer A (25 mM Tris 8.0, 5% glycerol) to 40% Buffer B (25 mM Tris 8.0, 1 M NaCl, 5% glycerol). The peak fractions were pooled, supplemented with 5 mM DTT, and further purified by Superdex 200 increase 10/300 GL column (GE Healthcare) and eluted by SEC buffer (25 mM HEPES 7.4, 150 mM NaCl). The peak fractions were pooled and concentrated for biochemical assays.

Gel filtration assay

Gel filtration assay was used to analyze the binding of PYL2-SHP1 to ABI-BCR::ABL1 in the presence of ABA. 100 μL of purified His-PYL2-SHP1 (10 μM) in SEC buffer (25 mM HEPES 7.4, 150 mM NaCl) was mixed with 100 μL of purified FLAG-ABI-BCR::ABL1 (1 μM) in SEC buffer, or with 100 μL of SEC buffer alone. The resulting 200 μL mixture was incubated with 100 μL of ABA (750 μM), which was prepared by diluting a 250 mM stock in DMSO using SEC buffer, or mixed with 100 μL of a DMSO control in SEC buffer at 4 °C for 4 hours. Each of these mixtures was subsequently subjected to gel filtration using the Superdex 200 increase 10/300 GL column (GE Healthcare). The eluted fractions were collected and analyzed by SDS-PAGE.

In vitro dephosphorylation assay of BCR::ABL1

Purified FLAG-ABI-BCR::ABL1 at a concentration of 0.6 μM in 25 mM HEPES pH 7.4, 150 mM NaCl was diluted to 60 nM using buffer K (50 mM HEPES pH 7.4, 150 mM NaCl, 0.01% Triton X-100, 0.01% BSA, 5 mM $MgCl_2$ and 2 mM DTT). Purified His-PYL2-SHP1 at a concentration of 10 μM in 25 mM HEPES pH 7.4, 150 mM NaCl was diluted to 120 nM using buffer K. ATP at pH 7.0 at a concentration of 100 mM in H_2O was diluted to 400 μM using buffer K. 150 μL of the diluted FLAG-ABI-BCR::ABL1 was mixed with 75 μL of the diluted His-PYL2-SHP1, then 75 μL of the diluted

ATP was added to initiate the phosphorylation reaction. The reaction was carried out at 30 °C in a metal bath. At time points of 0 min and 50 min, 12.5 μL of the reaction mixture was transferred to 2x SDS loading buffer and immediately heated at 95 °C for 5 min to stop the reaction.

After 50 min, 100 μL of the reaction mixture was mixed with 100 μL of 500 μM ABA that was prepared by dilution of a 250 mM stock in DMSO using buffer K, or mixed with 100 μL of a DMSO control in buffer K. At time points of additional 20 min and 50 min, 25 μL of the reaction mixture was removed and mixed with 2x SDS loading buffer and immediately heated at 95 °C for 5 min. The samples mixed with SDS loading buffer were then subjected to immunoblotting.

In vitro dephosphorylation assay of BRAF(V600E) and MEK

Purified His-BRAF(V600E)-ABI-FLAG at a concentration of 5 μM in 25 mM HEPES 7.4, 150 mM NaCl was diluted to 240 nM using buffer A (50 mM HEPES 7.4, 150 mM NaCl, 0.01% Triton X-100, 0.01% BSA, 2 mM $MgCl_2$, 2 mM DTT). MEK-His at a concentration of 56 μM in 25 mM HEPES 7.4, 150 mM NaCl was diluted to 1.2 μM using buffer A. ATP at pH 7.0 at a concentration of 100 mM in H_2O was diluted to 400 μM using buffer A. PP5-PYL2-FLAG at a concentration of 7 μM in 25 mM HEPES 7.4, 150 mM NaCl was diluted to 150 nM in buffer B (50 mM HEPES 7.4, 150 mM NaCl, 0.01% Triton X-100, 0.01% BSA, 100 μM $MnCl_2$, 2 mM DTT, 100 μM Palmitoyl-CoA) or buffer C (50 mM HEPES 7.4, 150 mM NaCl, 0.01% Triton X-100, 0.01% BSA, 1 mM $MnCl_2$, 2 mM DTT, 100 μM Palmitoyl-CoA). Palmitoyl-CoA was purchased from Sigma (Cat# P9716) and prepared as a 10 mM stock in H_2O. Dabrafenib (TargetMol, Cat# T1903) was prepared as a 10 mM stock in DMSO.

Firstly, 160 μL of the diluted His-BRAF(V600E)-ABI-FLAG was mixed with 160 μL of the diluted MEK-His. The kinase reaction was initiated by adding 320 μL of the diluted ATP and then carried out at 30 °C. At time points of 0 min and 30 min, 5 μL of the reaction mixture was removed and immediately mixed with 2x SDS loading buffer and heated at 95 °C for 5 min. Secondly, 250 μL of the reaction mixture was mixed with 250 μL of the diluted PP5-PYL2-FLAG in buffer B or C to initiate the dephosphorylation reaction. The reaction was carried out at 30 °C for 50 min, then 10 μL of the reaction mixture was removed and mixed with 2x SDS loading buffer and heated at 95 °C for 5 min. Thirdly, 384 μL of the remaining reaction mixture was transferred to four Eppendorf tubes (96 μL per tube); to each tube, 24 μL of ABA (1250 μM), 24 μL of Dabrafenib (50 μM), or 24 μL of ABA (1250 μM) plus Dabrafenib (50 μM), or 24 μL of a DMSO control, in buffer D (50 mM HEPES 7.4, 150 mM NaCl, 0.01% Triton X-100, 0.01% BSA, 1 mM $MgCl_2$, 50 μM $MnCl_2$, 2 mM DTT and 50 μM Palmitoyl-CoA) or in buffer E (50 mM HEPES 7.4, 150 mM NaCl, 0.01% Triton X-100, 0.01% BSA, 1 mM $MgCl_2$, 500 μM $MnCl_2$, 2 mM DTT and 50 μM Palmitoyl-CoA) was added. After additional 50 min, 12.5 μL of each reaction mixture was removed and mixed with 2x SDS loading buffer and heated at 95°C for 5 min.

The samples mixed with SDS loading buffer were subjected to immunoblotting. The bands on the immunoblotting image were quantified using ImageJ 1.53k.

Mass spectrometry

50 mL of the Ba/F3 cells stably expressing FLAG-tagged kinase-ABI or ABI-kinase fusion protein together with HA-tagged PYL2-phosphatase fusion protein, were treated with 50 μL of ABA (250 mM stock in DMSO) or 50 μL of DMSO for 12 h. Then the cells were pelleted by centrifugation (1,000 g, 2 min), washed twice with ice-cold PBS, lysed by incubating with 800 μL of the lysis buffer (25 mM Tris 8.0, 150 mM NaCl, 5% glycerol) supplemented with 1% Triton X-100, 1 mM EDTA, and protease inhibitors and phosphatase inhibitors at 4 °C for 1.5 h. The lysates were centrifuged at 22,000 g for 10 min. The protein concentration in the supernatant was determined by BCA protein assay. 70 μL of the supernatant was mixed with 2x SDS loading buffer, heated at 95 °C for 5 min and then subjected to immunoblotting.

About 700 μL of the supernatant was incubated with 50 μL of MonoRab™ Anti-DYKDDDDK Magnetic Beads (GeneScript, Cat# L00835-1) at 4 °C for 4 h, washed and eluted following the manufacturer's protocol. The eluate (about 200 μL) was mixed with 50 μL of 5x SDS loading buffer, separated by SDS-PAGE, and stained with Coomassie brilliant blue G-250. The gel bands of interest were cut into pieces. Proteins in the gel were reduced and alkylated in 50 mM ammonium bicarbonate at 37 °C overnight and then digested by trypsin. The digested products were extracted twice with 0.1% formic acid in 50% acetonitrile aqueous solution and dried by SpeedVac.

For LC-MS/MS analysis, the digested products were loaded into an analytical column made by packing C-18 resin (300 A, 3 μm, Varian, Lexington, MA) into a fused silica capillary column (75 μm ID, 150 mm length; Upchurch, Oak Harbor, WA), and then eluted by a linear gradient from 99% mobile phase A (0.1% formic acid in water) to 99% mobile phase B (80% acetonitrile and 0.1% formic acid) over 120 min (for the detection of protein phosphorylation) or 65 min (for the detection of phosphatases that were recruited to BRAF of MEK) with a flow rate of 0.300 μL/min in a Thermo Vanquish Neo integrated nano-HPLC system that was directly interfaced with a Thermo Exploris 480 mass spectrometer. The mass spectrometer was operated in the data-dependent acquisition mode using the Xcalibur 4.1 software. A single full-scan mass spectrum in the Orbitrap (350-1800 m/z, 60,000 resolution) was done followed by several data-dependent MS/MS scans at 30% normalized collision energy. The AGC target was set as 5e4, and the maximum injection time was 50 ms. Each mass spectrum was analyzed using the Thermo Xcalibur Qual Browser and Proteome Discoverer (2.5.0.400). The Sequest search parameters included a 10 ppm precursor mass tolerance, 0.02 Da fragment ion tolerance, and up to 2 internal cleavage sites. Cysteine alkylation was treated as fixed modification. Methionine oxidation and STY phosphorylation were treated as variable modifications. Peptides were filtered with 1% false discovery rate (FDR).

Statistics and reproducibility

The viability data in Figs. 3, 4, 5 and Supplementary Fig. 5b represent the mean ± SD of three or four independent measurements with technical duplicates were analyzed in GraphPad Prism 7. The western blot data in Fig. 7 represent the mean ± SD of five independent measurements and were analyzed using the unpaired *t*-test in Prism to calculate the two-tailed *P* values: $****P < 0.0001$; $***P < 0.001$; $**P < 0.01$; $*P < 0.05$.

Reporting summary

Further information on research design is available in the Nature Portfolio Reporting Summary linked to this article.

Data availability

Requests for resources and reagents should be directed to the lead contact, Qi Hu (huqi@westlake.edu.cn). All the data are available in the manuscript or the supplementary materials. The source data behind the graphs in the paper can be found in Supplementary Data. The uncropped and unedited blot/gel images in the paper can be found in Supplementary Fig. 7.

Received: 24 December 2023; Accepted: 22 August 2024;
Published online: 31 August 2024

References

1. Ardito, F., Giuliani, M., Perrone, D., Troiano, G. & Lo Muzio, L. The crucial role of protein phosphorylation in cell signaling and its use as targeted therapy (Review). *Int J. Mol. Med.* **40**, 271–280 (2017).
2. Manning, G., Whyte, D. B., Martinez, R., Hunter, T. & Sudarsanam, S. The protein kinase complement of the human genome. *Science* **298**, 1912–1934 (2002).
3. Chen, M. J., Dixon, J. E. & Manning, G. Genomics and evolution of protein phosphatases. *Sci. Signal* **10**, eaag1796 (2017).
4. Tsai, C. J. & Nussinov, R. The molecular basis of targeting protein kinases in cancer therapeutics. *Semin. Cancer Biol.* **23**, 235–242 (2013).
5. Benn, C. L. & Dawson, L. A. Clinically precedented protein kinases: rationale for their use in neurodegenerative disease. *Front Aging Neurosci.* **12**, 242 (2020).

6. Nikolic, I., Leiva, M. & Sabio, G. The role of stress kinases in metabolic disease. *Nat. Rev. Endocrinol.* **16**, 697–716 (2020).
7. Hantschel, O. & Superti-Furga, G. Regulation of the c-Abl and Bcr-Abl tyrosine kinases. *Nat. Rev. Mol. Cell Biol.* **5**, 33–44 (2004).
8. Bruford, E. A. et al. HUGO Gene Nomenclature Committee (HGNC) recommendations for the designation of gene fusions. *Leukemia* **35**, 3040–3043 (2021).
9. Lavoie, H. & Therrien, M. Regulation of RAF protein kinases in ERK signalling. *Nat. Rev. Mol. Cell Biol.* **16**, 281–298 (2015).
10. Lim, Y. M., Wong, S., Lau, G., Witte, O. N. & Colicelli, J. BCR/ABL inhibition by an escort/phosphatase fusion protein. *Proc. Natl. Acad. Sci. USA* **97**, 12233–12238 (2000).
11. Simpson, L. M. et al. An affinity-directed phosphatase, AdPhosphatase, system for targeted protein dephosphorylation. *Cell Chem. Biol.* **30**, 188–202.e186 (2023).
12. Sakamoto, K. M. et al. Protacs: chimeric molecules that target proteins to the Skp1-Cullin-F box complex for ubiquitination and degradation. *Proc. Natl. Acad. Sci. USA* **98**, 8554–8559 (2001).
13. Yamazoe, S. et al. Heterobifunctional molecules induce dephosphorylation of kinases-A proof of concept study. *J. Med Chem.* **63**, 2807–2813 (2020).
14. Zheng, J. et al. A novel dephosphorylation targeting chimera selectively promoting tau removal in tauopathies. *Signal Transduct. Target Ther.* **6**, 269 (2021).
15. Chen, P. H. et al. Modulation of phosphoprotein activity by phosphorylation targeting chimeras (PhosTACs). *ACS Chem. Biol.* **16**, 2808–2815 (2021).
16. Zhang, Q. et al. Protein phosphatase 5-recruiting chimeras for accelerating apoptosis-signal-regulated kinase 1 dephosphorylation with antiproliferative activity. *J. Am. Chem. Soc.* **145**, 1118–1128 (2023).
17. Stanton, B. Z., Chory, E. J. & Crabtree, G. R. Chemically induced proximity in biology and medicine. *Science* **359**, eaao5902 (2018).
18. Rivera, V. M. et al. A humanized system for pharmacologic control of gene expression. *Nat. Med.* **2**, 1028–1032 (1996).
19. Ueno, T., Falkenburger, B. H., Pohlmeyer, C. & Inoue, T. Triggering actin comets versus membrane ruffles: distinctive effects of phosphoinositides on actin reorganization. *Sci. Signal* **4**, ra87 (2011).
20. Putyrski, M. & Schultz, C. Protein translocation as a tool: the current rapamycin story. *FEBS Lett.* **586**, 2097–2105 (2012).
21. Liang, F. S., Ho, W. Q. & Crabtree, G. R. Engineering the ABA plant stress pathway for regulation of induced proximity. *Sci. Signal* **4**, rs2 (2011).
22. Warmuth, M., Kim, S., Gu, X. J., Xia, G. & Adrian, F. Ba/F3 cells and their use in kinase drug discovery. *Curr. Opin. Oncol.* **19**, 55–60 (2007).
23. Steelman, L. S. et al. JAK/STAT, Raf/MEK/ERK, PI3K/Akt and BCR-ABL in cell cycle progression and leukemogenesis. *Leukemia* **18**, 189–218 (2004).
24. ten Hoeve, J., Arlinghaus, R. B., Guo, J. Q., Heisterkamp, N. & Groffen, J. Tyrosine phosphorylation of CRKL in Philadelphia+ leukemia. *Blood* **84**, 1731–1736 (1994).
25. Capdeville, R., Buchdunger, E., Zimmermann, J. & Matter, A. Glivec (STI571, imatinib), a rationally developed, targeted anticancer drug. *Nat. Rev. Drug Discov.* **1**, 493–502 (2002).
26. Palombella, V. J., Rando, O. J., Goldberg, A. L. & Maniatis, T. The ubiquitin-proteasome pathway is required for processing the NF-kappa B1 precursor protein and the activation of NF-kappa B. *Cell* **78**, 773–785 (1994).
27. Janas, J. A. & Van Aelst, L. Oncogenic tyrosine kinases target Dok-1 for ubiquitin-mediated proteasomal degradation to promote cell transformation. *Mol. Cell Biol.* **31**, 2552–2565 (2011).
28. Shibata, N. et al. Development of protein degradation inducers of oncogenic BCR-ABL protein by conjugation of ABL kinase inhibitors and IAP ligands. *Cancer Sci.* **108**, 1657–1666 (2017).
29. Elgehama, A. et al. Targeting the PTP1B-Bcr-Abl1 interaction for the degradation of T315I mutant Bcr-Abl1 in chronic myeloid leukemia. *Cancer Sci.* **114**, 247–258 (2023).
30. Jeffrey, K. L., Camps, M., Rommel, C. & Mackay, C. R. Targeting dual-specificity phosphatases: manipulating MAP kinase signalling and immune responses. *Nat. Rev. Drug Discov.* **6**, 391–403 (2007).
31. Lee, Y. R., Chen, M. & Pandolfi, P. P. The functions and regulation of the PTEN tumour suppressor: new modes and prospects. *Nat. Rev. Mol. Cell Biol.* **19**, 547–562 (2018).
32. Khoubai, F. Z. & Grosset, C. F. DUSP9, a dual-specificity phosphatase with a key role in cell biology and human diseases. *Int J. Mol. Sci.* **22**, 11538 (2021).
33. Caunt, C. J. & Keyse, S. M. Dual-specificity MAP kinase phosphatases (MKPs): shaping the outcome of MAP kinase signalling. *FEBS J.* **280**, 489–504 (2013).
34. Foucquier, J. & Guedj, M. Analysis of drug combinations: current methodological landscape. *Pharm. Res. Perspect.* **3**, e00149 (2015).
35. McCubrey, J. A. et al. Roles of the Raf/MEK/ERK pathway in cell growth, malignant transformation and drug resistance. *Biochim. Biophys. Acta* **1773**, 1263–1284 (2007).
36. Ullah, R., Yin, Q., Snell, A. H. & Wan, L. RAF-MEK-ERK pathway in cancer evolution and treatment. *Semin Cancer Biol.* **85**, 123–154 (2022).
37. Davies, H. et al. Mutations of the BRAF gene in human cancer. *Nature* **417**, 949–954 (2002).
38. Holderfield, M., Deuker, M. M., McCormick, F. & McMahon, M. Targeting RAF kinases for cancer therapy: BRAF-mutated melanoma and beyond. *Nat. Rev. Cancer* **14**, 455–467 (2014).
39. Jaumot, M. & Hancock, J. F. Protein phosphatases 1 and 2A promote Raf-1 activation by regulating 14-3-3 interactions. *Oncogene* **20**, 3949–3958 (2001).
40. Mitsuhashi, S. et al. Usage of tautomycetin, a novel inhibitor of protein phosphatase 1 (PP1), reveals that PP1 is a positive regulator of Raf-1 in vivo. *J. Biol. Chem.* **278**, 82–88 (2003).
41. von Kriegsheim, A., Pitt, A., Grindlay, G. J., Kolch, W. & Dhillon, A. S. Regulation of the Raf-MEK-ERK pathway by protein phosphatase 5. *Nat. Cell Biol.* **8**, 1011–1016 (2006).
42. Brummer, T. et al. Functional analysis of the regulatory requirements of B-Raf and the B-Raf(V600E) oncoprotein. *Oncogene* **25**, 6262–6276 (2006).
43. Roring, M. et al. Distinct requirement for an intact dimer interface in wild-type, V600E and kinase-dead B-Raf signalling. *EMBO J.* **31**, 2629–2647 (2012).
44. Ritt, D. A., Monson, D. M., Specht, S. I. & Morrison, D. K. Impact of feedback phosphorylation and Raf heterodimerization on normal and mutant B-Raf signaling. *Mol. Cell Biol.* **30**, 806–819 (2010).
45. Fischer, A. et al. Regulation of RAF activity by 14-3-3 proteins: RAF kinases associate functionally with both homo- and heterodimeric forms of 14-3-3 proteins. *J. Biol. Chem.* **284**, 3183–3194 (2009).
46. Kohler, M. et al. Activation loop phosphorylation regulates B-Raf in vivo and transformation by B-Raf mutants. *EMBO J.* **35**, 143–161 (2016).
47. Roskoski, R. Jr Properties of FDA-approved small molecule protein kinase inhibitors: A 2023 update. *Pharm. Res.* **187**, 106552 (2023).
48. Bollag, G. et al. Vemurafenib: the first drug approved for BRAF-mutant cancer. *Nat. Rev. Drug Discov.* **11**, 873–886 (2012).
49. Poulikakos, P. I. et al. RAF inhibitor resistance is mediated by dimerization of aberrantly spliced BRAF(V600E). *Nature* **480**, 387–390 (2011).
50. Yaeger, R. et al. Mechanisms of acquired resistance to BRAF V600E inhibition in colon cancers converge on RAF dimerization and are sensitive to its inhibition. *Cancer Res.* **77**, 6513–6523 (2017).
51. Shimizu, Y. et al. Acquired resistance to BRAF inhibitors is mediated by BRAF splicing variants in BRAF V600E mutation-positive colorectal neuroendocrine carcinoma. *Cancer Lett.* **543**, 215799 (2022).
52. Caunt, C. J., Sale, M. J., Smith, P. D. & Cook, S. J. MEK1 and MEK2 inhibitors and cancer therapy: the long and winding road. *Nat. Rev. Cancer* **15**, 577–592 (2015).

53. Aoidi, R., Maltais, A. & Charron, J. Functional redundancy of the kinases MEK1 and MEK2: Rescue of the Mek1 mutant phenotype by Mek2 knock-in reveals a protein threshold effect. *Sci. Signal* **9**, ra9 (2016).
54. Haling, J. R. et al. Structure of the BRAF-MEK complex reveals a kinase activity independent role for BRAF in MAPK signaling. *Cancer Cell* **26**, 402–413 (2014).
55. Park, E. et al. Architecture of autoinhibited and active BRAF-MEK1-14-3-3 complexes. *Nature* **575**, 545–550 (2019).
56. Ramsey, A. J. & Chinkers, M. Identification of potential physiological activators of protein phosphatase 5. *Biochemistry* **41**, 5625–5632 (2002).
57. Swingle, M. R., Honkanen, R. E. & Ciszak, E. M. Structural basis for the catalytic activity of human serine/threonine protein phosphatase-5. *J. Biol. Chem.* **279**, 33992–33999 (2004).
58. Oberoi, J. et al. Structural and functional basis of protein phosphatase 5 substrate specificity. *Proc. Natl. Acad. Sci. USA* **113**, 9009–9014 (2016).
59. Ash, D. E. & Schramm, V. L. Determination of free and bound manganese(II) in hepatocytes from fed and fasted rats. *J. Biol. Chem.* **257**, 9261–9264 (1982).
60. Emuss, V., Garnett, M., Mason, C. & Marais, R. Mutations of C-RAF are rare in human cancer because C-RAF has a low basal kinase activity compared with B-RAF. *Cancer Res.* **65**, 9719–9726 (2005).
61. Hu, J. et al. Kinase regulation by hydrophobic spine assembly in cancer. *Mol. Cell Biol.* **35**, 264–276 (2015).
62. Oberoi, J. et al. HSP90-CDC37-PP5 forms a structural platform for kinase dephosphorylation. *Nat. Commun.* **13**, 7343 (2022).
63. Vido, M. J., Rock, J. & Aplin, A. E. Role of serine 365 in BRAF V600E sensitivity to RAF inhibition. *Pigment Cell Melanoma Res.* **34**, 696–702 (2021).
64. Diedrich, B. et al. Discrete cytosolic macromolecular BRAF complexes exhibit distinct activities and composition. *EMBO J.* **36**, 646–663 (2017).

Acknowledgements

We thank Dr. Hongtao Yu for helpful comments, the reviewers for their constructive feedback, and the Mass Spectrometry & Metabolomics Core Facility at the Center for Biomedical Research Core Facilities of Westlake University for sample analysis. This work was supported by the "Pioneer" and "Leading Goose" R&D Program of Zhejiang (2023C03109, 2024SSYS0036), and Westlake Education Foundation.

Author contributions

Q.H. conceived the project. Y.S. and R.Z. purified the proteins. Y.S. designed and performed all the assays. J.H. and S.F. performed the MS experiments and analyzed the data. Y.S. and Q.H. analyzed the data and wrote the manuscript.

Competing interests

The authors declare no competing interests.

Additional information

Supplementary information The online version contains supplementary material available at https://doi.org/10.1038/s42003-024-06771-9.

Correspondence and requests for materials should be addressed to Qi Hu.

Peer review information *Communications Biology* thanks the anonymous reviewers for their contribution to the peer review of this work. Primary Handling Editor: Ophelia Bu. [A peer review file is available.]